

Decentralized Adversarial Training over Graphs

Ying Cao, Elsa Rizk, Stefan Vlaski, *Member, IEEE*, Ali H. Sayed, *Fellow, IEEE*

Abstract—The vulnerability of machine learning models to adversarial attacks has been attracting considerable attention in recent years. Most existing studies focus on the behavior of stand-alone single-agent learners. In comparison, this work studies adversarial training over graphs, where individual agents are subjected to perturbations of varied strength levels across space. It is expected that interactions by linked agents, and the heterogeneity of the attack models that are possible over the graph, can help enhance robustness in view of the coordination power of the group. Using a min-max formulation of diffusion learning, we develop a decentralized adversarial training framework for multi-agent systems. We analyze the convergence properties of the proposed scheme for both convex and non-convex environments, and illustrate the enhanced robustness to adversarial attacks.

Index Terms—robustness, adversarial training, decentralized setting, diffusion strategy, multi-agent system.

I. INTRODUCTION

In many machine learning algorithms, small malicious perturbations that are imperceptible to the human eye can cause classifiers to reach erroneous conclusions [2]–[4]. This sensitivity is problematic for important applications, such as computer vision [5], [6], natural language processing [7], [8], and reinforcement learning [9]. Several defense mechanisms have been proposed in the literature [10]–[14] to mitigate the negative effect of adversarial examples, including the popular scheme based on adversarial training [14]. In this approach, clean training samples are augmented by adding purposefully crafted perturbations. Due to the lack of an explicit definition for the imperceptibility of perturbations, additive attacks are usually restricted within a small bounded region.

Most earlier studies, such as [7], [14]–[17], focus on studying adversarial training in the context of single agent learning. However, distributed settings, which consist of a group of agents, are becoming more prevalent in a highly connected world [18], [19]. Examples abound in transportation networks, communication networks and biological networks. In this work, we devise a robust training algorithm for multi-agent networked systems by relying on diffusion learning [4], [19], [20], which has been shown to have a wider stability range and improved performance guarantees for adaptation in comparison to other decentralized strategies [4], [19], [20].

There of course exist other works in the literature that have applied adversarial learning to a multiplicity of agents, albeit using a different architecture. For example, the works [21]–[23] employ multiple GPUs and a fusion center, while

the works [24]–[26] consider graph neural networks. In this work, we focus on a fully decentralized architecture where each agent corresponds to a learning unit in its own right, and interactions occur locally over neighborhoods determined by a graph topology.

The contributions of this work are listed as follows:

(1) We formulate a sequential minimax optimization problem involving adversarial samples, where the perturbations are within some general ℓ_p norm-bounded region. To solve the problem, we propose a decentralized framework based on diffusion learning, where all agents are subjected to adversarial examples and work together through local interactions to defend the network globally. Although we motivate our framework by focusing on stochastic gradient implementations, we hasten to add that other more complex optimizers can be used as well.

(2) In the performance analysis, we examine the convergence of the proposed framework for both cases of convex and non-convex optimization environments. In particular, we show that for strongly-convex loss functions, and despite the perturbations, the proposed algorithm is able to approach the global minimizer within $O(\mu)$ after sufficient iterations, where μ is the step-size parameter. In comparison, for non-convex losses, the algorithm is guaranteed to converge to a point that is $O(\mu) + O(\epsilon^2)$ close to an approximate stationary point of the global objective function, where ϵ is the maximum perturbation bound over the entire graph. Our results are more general than some earlier investigations in the literature where the loss function in the inner maximization step is required to be concave [22], [27], [28].

(3) In the simulations, we illustrate how the robustness of the multi-agent systems can be improved by the proposed framework. We simulate both the convex and non-convex environments, and both homogeneous and heterogeneous networks. We show how the adversarial diffusion strategy enables more robust behavior than non-cooperative and even centralized methods in the non-convex environments. This fact demonstrates the role of the graph topology in resisting adversarial settings.

II. PROBLEM FORMULATION

We consider a collection of K agents over a graph, where each agent k observes independent realizations of some random data $(\mathbf{x}_k, \mathbf{y}_k)$, in which \mathbf{x}_k plays the role of the feature vector and \mathbf{y}_k plays the role of the label variable. Adversarial learning in the heterogeneous decentralized setting deals with

A short version of this work without proofs and focusing only on the convex case appears in the conference publication [1].

Ying Cao, Elsa Rizk, Ali H. Sayed are with the School of Engineering, École Polytechnique Fédérale de Lausanne. Stefan Vlaski is with the Department of Electrical and Electronic Engineering, Imperial College London. Emails: {ying.cao, elsa.rizk, ali.sayed}@epfl.ch, s.vlaski@imperial.ac.uk.

the following stochastic minimax optimization problem:

$$w^* = \operatorname{argmin}_{w \in \mathbb{R}^M} \left\{ J(w) \triangleq \sum_{k=1}^K \pi_k J_k(w) \right\} \quad (1)$$

where M is the dimension of the feature vectors, $\{\pi_k\}_{k=1}^K$ are positive scaling weights adding up to one, and each individual risk function is defined by

$$J_k(w) = \mathbb{E}_{\{\mathbf{x}_k, \mathbf{y}_k\}} \left\{ \max_{\|\delta_k\|_{p_k} \leq \epsilon_k} Q_k(w; \mathbf{x}_k + \delta_k, \mathbf{y}_k) \right\} \quad (2)$$

in terms of a loss function $Q_k(\cdot)$. In this formulation, \mathbf{y}_k is the true label of sample \mathbf{x}_k , and the variable δ_k represents a norm-bounded perturbation added to the clean sample. In this paper, we assume all agents observe independently and identically distributed (i.e., iid) data over time, but allow for non-iid samples over space. The type of the norm p_k and the upper bound ϵ_k are allowed to vary across agents, thus leading to the possibility of heterogeneous models over the graph. In particular, ℓ_2 and ℓ_∞ norms are among two of the possible choices for which the results of this paper hold. We refer to w^* as the *robust model* since it relies on the worst-case perturbation found from (2).

One methodology for solving (1) is to first determine the inner maximizer in (2), thus reducing the minimax problem to a standard stochastic minimization formulation. Then, the traditional stochastic gradient method could be used to seek the minimizer. We denote the true maximizer of the perturbed loss function in (2) by

$$\delta_k^*(w) \in \operatorname{argmax}_{\|\delta_k\|_{p_k} \leq \epsilon_k} Q_k(w; \mathbf{x}_k + \delta_k, \mathbf{y}_k) \quad (3)$$

where the dependence of δ_k^* on w is shown explicitly. We use the boldface notation for $\delta_k^*(w)$ because it is now a function of the random data $(\mathbf{x}_k, \mathbf{y}_k)$. To apply the stochastic gradient method, we would need to evaluate the gradient of $Q(w; \mathbf{x}_k + \delta_k^*(w), \mathbf{y}_k)$ relative to w , which can be challenging since $\delta_k^*(w)$ is also dependent on w . Fortunately, this difficulty can be resolved by appealing to Danskin's theorem – see section 6.11 in [29] and section B.5 in [30]. Let

$$g(w) \triangleq \max_{\|\delta_k\|_{p_k} \leq \epsilon_k} Q_k(w; \mathbf{x}_k + \delta_k, \mathbf{y}_k) \quad (4)$$

Then, the theorem asserts that $g(w)$ is convex over w if $Q_k(w; \cdot, \cdot)$ is convex over w . However, $g(w)$ need not be differentiable over w even when $Q_k(w; \cdot, \cdot)$ is differentiable. Nevertheless, and importantly for our purposes, we can determine a subgradient for $g(w)$ by using the actual gradient of the loss evaluated at the worst perturbation, namely, it holds that

$$\nabla_w Q_k(w; \mathbf{x}_k + \delta_k^*, \mathbf{y}_k) \in \partial_w g(w) \quad (5)$$

where ∂_w refers to the subdifferential set of its argument. In (5), the gradient of $Q_k(\cdot)$ relative to w is computed by treating δ_k^* as a stand-alone vector and ignoring its dependence on w . When δ_k^* in (3) happens to be *unique*, then the gradient on

the left in (5) will be equal to the right side, so that in that case the function $g(w)$ will be *differentiable*.

Motivated by these properties, and using (5), we can now devise an algorithm to enhance the robustness of multi-agent systems to adversarial perturbations. To do so, we rely on the adapt-then-combine (ATC) version of the diffusion strategy [4], [19] and write down the mini-batch adversarial extension to solve (1)–(2). The details can be found in the listing of Algorithm 1, where

$$\delta_{k,n}^{b,*} \in \operatorname{argmax}_{\|\delta_k\|_{p_k} \leq \epsilon_k} Q_k(\mathbf{w}_{k,n-1}; \mathbf{x}_{k,n}^b + \delta_k, \mathbf{y}_{k,n}^b) \quad (6)$$

computes the perturbation for each sample from the mini batch at iteration n , and $\phi_{k,n}$ is the intermediate state obtained by performing a stochastic gradient step. The intermediate states $\phi_{\ell,n}$ from the neighbors of agent k are combined together using the scalars $a_{\ell k}$, which are non-negative and add to one over $\ell \in \mathcal{N}_k$.

Algorithm 1 : Adversarial diffusion training (ADT).

Input: Step size μ , batch size B , combination matrix A .

Output: A group of robust models $\{w_{k,N}\}_{k=0}^K$.

Initialize models for all agents at $\{w_{k,0}\}_{k=0}^K$.

for Iteration $n = 1 \rightarrow N$ **do**

for Agent $k = 1 \rightarrow K$ **do**

 Select mini-batch training samples $\{\mathbf{x}_{k,n}^b, \mathbf{y}_{k,n}^b\}_{b=1}^B$.

for $b = 1 \rightarrow B$ **do**

 Construct $\delta_{k,n}^{b,*}$ using (6)

$$\mathbf{x}_{k,n}^{b,*} = \mathbf{x}_{k,n}^b + \delta_{k,n}^{b,*}$$

end for

$$\phi_{k,n} = \mathbf{w}_{k,n-1} - \frac{\mu}{B} \sum_{b=1}^B \nabla_w Q_k(\mathbf{w}_{k,n-1}; \mathbf{x}_{k,n}^{b,*}, \mathbf{y}_{k,n}^b)$$

end for

$$\mathbf{w}_{k,n} = \sum_{\ell \in \mathcal{N}_k} a_{\ell k} \phi_{\ell,n}$$

end for

We still need to compute the exact inner maximizer $\delta_{k,n}^{b,*}$ in (6), and this step will be discussed for convex and non-convex environments separately in this paper. But first we list the following assumptions for both convex and non-convex cases, which are commonly used in the literature of decentralized multi-agent learning, as well as in works on single-agent adversarial training [4], [20], [27], [31], [32].

First, it is necessary to define the combination matrix A according to which the agents interact over the graph topology.

Assumption 1. (Strongly-connected graph) *The entries of the combination matrix $A = [a_{\ell k}]$ satisfy $a_{\ell k} \geq 0$ and the entries on each column add up to one, which means that A is left-stochastic. Moreover, the graph is strongly-connected, meaning that there exists a path with nonzero weights $\{a_{\ell k}\}$ linking any pair of agents and, in addition, at least one node k in the network has a self-loop with $a_{kk} > 0$.* □

It follows from the Perron-Frobenius theorem [4], [20] that A has a single eigenvalue at 1. Let $\pi = \{\pi_k\}_{k=1}^K$ be the

corresponding right eigenvector of A . It then follows from the same theorem that we can normalize the entries of π to satisfy:

$$A\pi = \pi, \quad \mathbb{1}^\top \pi = 1, \quad \pi_k > 0 \quad (7)$$

Next, we require the loss function Q_k at each agent to be smooth, which is a common assumption in the field of min-max optimization and adversarial learning [27], [30], [33].

Assumption 2. (Smooth loss functions) For each agent k , the gradients of the loss function relative to w and x are Lipschitz in relation to the variables $\{w, x, y\}$. More specifically, it holds that

$$\|\nabla_w Q_k(w_2; x + \delta, y) - \nabla_w Q_k(w_1; x + \delta, y)\| \leq L_1 \|w_2 - w_1\| \quad (8a)$$

$$\|\nabla_w Q_k(w; x_2 + \delta, y) - \nabla_w Q_k(w; x_1 + \delta, y)\| \leq L_2 \|x_2 - x_1\| \quad (8b)$$

$$\|\nabla_w Q_k(w; x + \delta, y_2) - \nabla_w Q_k(w; x + \delta, y_1)\| \leq L_3 \|y_2 - y_1\| \quad (8c)$$

and

$$\|\nabla_x Q_k(w_2; x + \delta, y) - \nabla_x Q_k(w_1; x + \delta, y)\| \leq L_4 \|w_2 - w_1\| \quad (9a)$$

$$\|\nabla_x Q_k(w; x_2 + \delta, y) - \nabla_x Q_k(w; x_1 + \delta, y)\| \leq L_5 \|x_2 - x_1\| \quad (9b)$$

with $\|\delta\|_{p_k} \leq \epsilon_k$. To simplify the notation, we let

$$L = \max\{L_1, L_2, L_3, L_4, L_5\}. \quad (10)$$

□

III. ANALYSIS IN CONVEX ENVIRONMENTS

This section analyzes the convergence of adversarial diffusion algorithm for the case of strongly convex loss functions. Besides Assumptions 1 and 2, we consider the following assumptions for the convex environment.

Assumption 3. (Strong convexity) For each agent k , the loss function $Q_k(w; \cdot)$ is ν -strongly convex over w , namely, for any $w_1, w_2, x \in \mathbb{R}^M$ and $y \in \mathbb{R}$, it holds that

$$Q_k(w_2; x, y) \geq Q_k(w_1; x, y) + \nabla_{w^\top} Q_k(w_1; x, y)(w_2 - w_1) + \frac{\nu}{2} \|w_2 - w_1\|^2 \quad (11)$$

□

We remark that it also follows from Danskin's theorem [30], [33], [34] that, when $Q_k(w; \cdot, \cdot)$ is ν -strongly convex over w , then the adversarial risk $J_k(w)$ defined by (2) will be strongly convex. As a result, the aggregate risk $J(w)$ in (1) will be strongly-convex as well.

Assumption 4. (Bounded gradient disagreement) For any pair of agents k and ℓ , the squared gradient disagreements are uniformly bounded on average, namely, for any $w, \delta \in \mathbb{R}^M$, it holds that

$$\mathbb{E}_{\{x, y\}} \|\nabla_w Q_k(w; x + \delta, y) - \nabla_w Q_\ell(w; x + \delta, y)\|^2 \leq C^2 \quad (12)$$

for any $\|\delta\|_{p_k} \leq \epsilon_k, \|\delta\|_{p_\ell} \leq \epsilon_\ell$.

□

This assumption is similar to the one used in [31], [32], and is automatically satisfied when all agents use the same loss function, or in the centralized case where only a single agent is considered.

To evaluate the performance of the adversarial diffusion algorithm, it is critical to compute the inner maximizer $\delta_{k,n}^{b,*}$ defined by (6). Fortunately, for some convex problems involving the logistic loss, the quadratic loss, and the exponential loss, the maximization in (6) has a *unique* closed-form solution (e.g., we will show this for the logistic loss in a later section). This uniqueness property enables us to analyze the convergence properties of the algorithm. We first establish the following affine Lipschitz result for the risk function in (2). The proof can be found in Appendix A.

Lemma 1. (Affine Lipschitz) For each agent k , the gradient of $J_k(w)$ is affine Lipschitz, namely, for any $w_1, w_2 \in \mathbb{R}^M$, it holds that

$$\|\nabla_w J_k(w_2) - \nabla_w J_k(w_1)\|^2 \leq 2L^2 \|w_2 - w_1\|^2 + O(\epsilon_k^2) \quad (13)$$

□

Contrary to the traditional analysis of decentralized learning algorithms where the risk functions $J_k(w)$ are generally Lipschitz, it turns out that under adversarial perturbations, the risks in (2) are now *affine* Lipschitz as shown by (13) due to the additional term $O(\epsilon_k^2)$. This fact requires adjustments to the convergence arguments. A similar situation arises, for example, when we study the convergence of decentralized learning under non-smooth losses and clean environments — see [4], [35].

To proceed with the convergence analysis, we introduce the gradient noise process, which is defined by

$$s_{k,n} \triangleq \nabla_w Q_k(w_{k,n-1}; \mathbf{x}_{k,n}^*, \mathbf{y}_{k,n}) - \nabla_w J_k(w_{k,n-1}) \quad (14)$$

This quantity measures the difference between the approximate gradient (represented by the gradient of the loss) and the true gradient (represented by the gradient of the risk) at iteration n . Similarly, we define the gradient noise for the mini-batch version as

$$\mathbf{s}_{k,n}^B \triangleq \frac{1}{B} \sum_{b=1}^B \nabla_w Q_k(w_{k,n-1}; \mathbf{x}_{k,n}^{b,*}, \mathbf{y}_{k,n}^b) - \nabla_w J_k(w_{k,n-1}) \quad (15)$$

The following result establishes some useful properties for the gradient noise process, namely, it has zero mean and bounded second-order moment (conditioned on past history), for which proofs can be found in Appendix B.

Lemma 2. (Moments of gradient noise) For each agent k , the gradient noise defined in (15) has zero mean and its variance is bounded:

$$\mathbb{E} \{ \mathbf{s}_{k,n}^B | \mathcal{F}_{n-1} \} = 0 \quad (16)$$

$$\mathbb{E} \left\{ \|\mathbf{s}_{k,n}^B\|^2 | \mathcal{F}_{n-1} \right\} \leq \beta_k^2 \|\tilde{\mathbf{w}}_{k,n-1}\|^2 + \sigma_k^2 \quad (17)$$

for some non-negative scalars given by

$$\begin{aligned}\beta_k^2 &= \frac{16L^2}{B} \\ \sigma_k^2 &= \frac{8}{B} \mathbb{E} \|\nabla_w Q_k(w^*; \mathbf{x}_{k,n} + \boldsymbol{\delta}_k^*(w^*), \mathbf{y}_{k,n})\|^2 + O(\epsilon_k^2)\end{aligned}\quad (18)$$

where

$$\boldsymbol{\delta}_k^*(w^*) = \operatorname{argmax}_{\|\delta\|_{p_k} \leq \epsilon_k} Q_k(w^*; \mathbf{x}_{k,n} + \delta, \mathbf{y}_{k,n}) \quad (19)$$

The quantity \mathcal{F}_{n-1} is the filtration generated by the past history of the random process $\operatorname{col}\{\mathbf{w}_{k,j}\}_{k=1}^K$ for $j \leq n-1$, and

$$\tilde{\mathbf{w}}_{k,n-1} \triangleq w^* - \mathbf{w}_{k,n-1} \quad (20)$$

□

To enable network analysis, we collect the error vectors from all agents into the $K \times 1$ block column vector:

$$\tilde{\mathbf{w}}_n \triangleq \operatorname{col}\{\tilde{\mathbf{w}}_{k,n}\}_{k=1}^K \quad (21)$$

Similarly, we gather the true gradients and the gradient noise from all agents into:

$$\nabla J(\mathbf{w}_{n-1}) \triangleq \operatorname{col}\{\nabla_w J_k(\mathbf{w}_{k,n-1})\} \quad (22)$$

$$\mathbf{s}_n^B \triangleq \operatorname{col}\{\mathbf{s}_{k,n}^B\} \quad (23)$$

Using these variables, the recursions of the adversarial diffusion training algorithm can be rewritten as

$$\tilde{\mathbf{w}}_n = \mathcal{A}^\top (\tilde{\mathbf{w}}_{n-1} + \mu \nabla J(\mathbf{w}_{n-1}) + \mathbf{s}_n^B) \quad (24)$$

where

$$\mathcal{A} = A \otimes I_M \quad (25)$$

and I_M is the identity matrix of size M , while \otimes denotes the Kronecker product operation. We exploit the eigen-structure of A by noting that the $K \times K$ matrix A admits a Jordan canonical decomposition of the form [20]:

$$A = V_\alpha J V_\alpha^{-1} \quad (26)$$

where the matrices $\{V_\alpha, J\}$ are

$$V_\alpha = [\pi \quad V_R], \quad J = \begin{bmatrix} 1 & 0 \\ 0 & J_\alpha \end{bmatrix}, \quad V_\alpha^{-1} = \begin{bmatrix} \mathbb{1}^\top \\ V_L^\top \end{bmatrix} \quad (27)$$

Here, J_α is a block Jordan matrix with eigenvalues from the second largest eigenvalue λ_2 to the smallest eigenvalue λ_K of A appearing on the diagonal and the positive scalar α , which can be chosen arbitrarily small, appearing on the first lower sub-diagonal. Then, the extended matrix \mathcal{A} satisfies

$$\mathcal{A} = V_\alpha \mathcal{J} V_\alpha^{-1} \quad (28)$$

where

$$V_\alpha = V_\alpha \otimes I_M, \quad \mathcal{J} = J \otimes I_M, \quad V_\alpha^{-1} = V_\alpha^{-1} \otimes I_M \quad (29)$$

Since

$$V_\alpha V_\alpha^{-1} = V_\alpha^{-1} V_\alpha = I_K \quad (30)$$

we have

$$\pi \mathbb{1}^\top + V_R V_L^\top = \mathbb{1} \pi^\top + V_L V_R^\top = I_K \quad (31a)$$

$$V_L^\top V_R = I_{K-1} \quad (31b)$$

$$V_L^\top \pi = \mathbb{1}^\top V_R = 0 \quad (31c)$$

Multiplying the error recursion (24) from the left by V_α^\top , and substituting (28) into it, we obtain the following recursion by following a similar derivation to [20], [36]:

$$\begin{aligned}V_\alpha^\top \tilde{\mathbf{w}}_n &= \begin{bmatrix} (\pi^\top \otimes I_M) \tilde{\mathbf{w}}_n \\ (V_R^\top \otimes I_M) \tilde{\mathbf{w}}_n \end{bmatrix} \triangleq \begin{bmatrix} \bar{\mathbf{w}}_n \\ \check{\mathbf{w}}_n \end{bmatrix} \\ &= \mathcal{J}^\top V_\alpha^\top (\tilde{\mathbf{w}}_{n-1} + \mu \nabla J(\mathbf{w}_{n-1}) + \mu \mathbf{s}_n^B) \\ &= \begin{bmatrix} I_M & \mathbf{0} \\ \mathbf{0} & J_\alpha^\top \otimes I_M \end{bmatrix} \begin{bmatrix} \bar{\mathbf{w}}_{n-1} \\ \check{\mathbf{w}}_{n-1} \end{bmatrix} + \\ &\quad \mu \begin{bmatrix} I_M & \mathbf{0} \\ \mathbf{0} & J_\alpha^\top \otimes I_M \end{bmatrix} \begin{bmatrix} \pi^\top \otimes I_M \\ V_R^\top \otimes I_M \end{bmatrix} \left(\nabla J(\mathbf{w}_{n-1}) + \mathbf{s}_n^B \right)\end{aligned}\quad (32)$$

It follows that we can split (24) into the following two recursions in terms of the transformed quantities $\{\bar{\mathbf{w}}_n, \check{\mathbf{w}}_n\}$:

$$\begin{aligned}\bar{\mathbf{w}}_n &= \sum_k \pi_k \tilde{\mathbf{w}}_{k,n-1} \\ &= \bar{\mathbf{w}}_{n-1} + \mu \sum_k \pi_k \nabla_w J_k(\mathbf{w}_{k,n-1}) + \mu \sum_k \pi_k \mathbf{s}_{k,n}^B\end{aligned}\quad (33)$$

and

$$\check{\mathbf{w}}_n = \mathcal{J}_\alpha^\top \check{\mathbf{w}}_{n-1} + \mu \mathcal{J}_\alpha^\top V_R^\top \nabla_w J(\mathbf{w}_{n-1}) + \mu \mathcal{J}_\alpha^\top V_R^\top \mathbf{s}_n^B \quad (34)$$

where

$$\mathcal{J}_\alpha = J_\alpha \otimes I_M, \quad V_R = V_R \otimes I_M \quad (35)$$

The convergence results for (33) and (34) are stated next, for which proofs can be found in Appendix C.

Theorem 1. (Network mean-square-error stability) Consider a network of K agents running the adversarial diffusion strategy from Algorithm 1. Under Assumptions 1–4 and for sufficiently small step-sizes μ , it holds that

$$\limsup_{n \rightarrow \infty} \mathbb{E} \|\check{\mathbf{w}}_n\|^2 \leq O(\mu^2), \quad \limsup_{n \rightarrow \infty} \mathbb{E} \|\bar{\mathbf{w}}_n\|^2 \leq O(\mu) \quad (36)$$

More specifically, the network converges asymptotically to a small neighborhood of the global minimizer w^* at an exponential rate:

$$\limsup_{n \rightarrow \infty} \mathbb{E} \|\tilde{\mathbf{w}}_n\|^2 \leq O(\lambda^n) + O(\mu) \quad (37)$$

where

$$\lambda = 1 - 2\nu\mu + O(\mu^2) \quad (38)$$

□

The above theorem indicates that the proposed algorithm

enables the network to approach in the mean-square-error sense an $O(\mu)$ -neighborhood of the robust minimizer w^* after enough iterations, so that the average worst-case performance over all possible perturbations in the small region bounded by ϵ_k is effectively minimized.

IV. ANALYSIS IN NON-CONVEX ENVIRONMENTS

For nonconvex losses, it is generally not possible to obtain closed form expressions for the maximizer $\delta_k^{b,*}$. Instead, one is satisfied with some common approximations for it [7], [14], [16]. One popular strategy is to resort to a first-order Taylor expansion for each agent around \mathbf{x}_k as follows:

$$\begin{aligned} Q_k(\mathbf{w}_k; \mathbf{x}_k + \delta_k, \mathbf{y}_k) \\ \approx Q_k(\mathbf{w}_k; \mathbf{x}_k, \mathbf{y}_k) + \delta_k^\top \nabla_x Q_k(\mathbf{w}_k; \mathbf{x}_k, \mathbf{y}_k) \end{aligned} \quad (39)$$

from which the following approximate maximizer can be derived:

$$\begin{aligned} \widehat{\delta}_k &= \operatorname{argmax}_{\|\delta_k\|_{p_k} \leq \epsilon_k} \left\{ Q_k(\mathbf{w}_k; \mathbf{x}_k, \mathbf{y}_k) + \delta_k^\top \nabla_x Q_k(\mathbf{w}_k; \mathbf{x}_k, \mathbf{y}_k) \right\} \\ &= \operatorname{argmax}_{\|\delta_k\|_{p_k} \leq \epsilon_k} \delta_k^\top \nabla_x Q_k(\mathbf{w}_k; \mathbf{x}_k, \mathbf{y}_k) \end{aligned} \quad (40)$$

Note that different choices for the p_k norm lead to different expressions for the approximate maximizer. For instance, when $p_k = 2$, we get:

$$\widehat{\delta}_k = \epsilon_k \frac{\nabla_x Q_k(\mathbf{w}_k; \mathbf{x}_k, \mathbf{y}_k)}{\|\nabla_x Q_k(\mathbf{w}_k; \mathbf{x}_k, \mathbf{y}_k)\|} \quad (41)$$

which motivates the fast gradient method (FGM) [7] in single-agent learning, while for $p = \infty$ we have

$$\widehat{\delta}_k = \epsilon_k \operatorname{sign} \left(\nabla_x Q_k(\mathbf{w}_k; \mathbf{x}_k, \mathbf{y}_k) \right) \quad (42)$$

which relates to the fast gradient sign method (FGSM) [15]. Moreover, depending on the number of iterations used when generating perturbations, the first-order gradient based methods include single-step attacks, such as FGM and FGSM, and multi-step ones, such as projected gradient descent (PGD). Although the latter perturbation has been empirically shown to be stronger than the former ones [14] and leads to more robust models, its computational complexity is also much higher [37]. In the simulations we use single-step methods, while noting that our framework can also be combined with multi-step attacks if necessary.

The above discussion motivates us to consider the following adversarial extension of the diffusion strategy for non-convex environments:

$$\widehat{\mathbf{x}}_{k,n}^b = \mathbf{x}_{k,n}^b + \widehat{\delta}_{k,n}^b \quad (43a)$$

$$\phi_{k,n} = \mathbf{w}_{k,n-1} - \frac{\mu}{B} \sum_{b=1}^B \nabla_w Q_k(\mathbf{w}_{k,n-1}; \widehat{\mathbf{x}}_{k,n}^b, \mathbf{y}_{k,n}^b) \quad (43b)$$

$$\mathbf{w}_{k,n} = \sum_{\ell \in \mathcal{N}_k} a_{\ell k} \phi_{\ell,n} \quad (43c)$$

In these expressions, the approximate maximizer $\widehat{\delta}_{k,n}^b$ replaces the exact $\delta_{k,n}^{b,*}$ in Algorithm 1. In other words, we consider the

same framework for both convex and non-convex cases, but different methods are implemented to compute the adversarial examples.

To analyze the performance of (43a)–(43c), we assume the following conditions concerning non-convex loss functions. First, we suppose that the expected norm of the gradient of $Q_k(\cdot)$ over w is bounded, which is common in non-convex optimization [27], [33], [38].

Assumption 5. (Bounded gradients) For each agent k , the expectation of the norm of the gradient $\nabla_w Q_k(w; \mathbf{x}_k + \delta_k, \mathbf{y}_k)$ is bounded, namely, for any $w \in \mathbb{R}^M$:

$$\mathbb{E} \|\nabla_w Q_k(w; \mathbf{x}_k + \delta_k, \mathbf{y}_k)\| \leq G \quad (44)$$

with $\|\delta_k\|_{p_k} \leq \epsilon_k$. □

Recall that according to Danskin’s theorem, the function $g(w)$ defined in (4) is not necessarily differentiable if the inner maximizer $\delta_k^{b,*}$ is not unique. It then follows that $J(w)$ defined by (1) is also not necessarily differentiable. To enable the analysis of (43a)–(43c), we introduce the following proxy for the “gradient” operator:

$$\overline{\nabla_w J_k}(\mathbf{w}_{k,n-1}) \triangleq \mathbb{E} \{ \nabla_w Q_k(\mathbf{w}_{k,n-1}; \widehat{\mathbf{x}}_{k,n}, \mathbf{y}_{k,n}) \} \quad (45)$$

which is the expectation of the gradient of $Q_k(\cdot)$ evaluated at the *approximate* maximizer. Then, similar to the convex case, we introduce the gradient noise to measure the difference between the stochastic gradient and the proxy gradient as follows:

$$\bar{\mathbf{s}}_{k,n}(\mathbf{w}_{k,n-1}) \triangleq \nabla_w Q_k(\mathbf{w}_{k,n-1}; \widehat{\mathbf{x}}_{k,n}, \mathbf{y}_{k,n}) - \overline{\nabla_w J_k}(\mathbf{w}_{k,n-1}) \quad (46)$$

It can be easily shown that the gradient of Q_k at one sample is an unbiased estimate of its expectation over all samples. That is,

$$\begin{aligned} \mathbb{E} \{ \bar{\mathbf{s}}_{k,n}(\mathbf{w}_{k,n-1}) | \mathcal{F}_{n-1} \} &= \mathbb{E} \left\{ \nabla_w Q_k(\mathbf{w}_{k,n-1}; \widehat{\mathbf{x}}_{k,n}, \mathbf{y}_{k,n}) \right. \\ &\quad \left. - \mathbb{E} \{ \nabla_w Q_k(\mathbf{w}_{k,n-1}; \widehat{\mathbf{x}}_{k,n}, \mathbf{y}_{k,n}) | \mathcal{F}_{n-1} \} \right\} = 0 \end{aligned} \quad (47)$$

Similarly, the gradient noise for the mini-batch version is defined by

$$\bar{\mathbf{s}}_{k,n}^B \triangleq \frac{1}{B} \sum_{b=1}^B \nabla_w Q_k(\mathbf{w}_{k,n-1}; \widehat{\mathbf{x}}_{k,n}^b, \mathbf{y}_{k,n}^b) - \overline{\nabla_w J_k}(\mathbf{w}_{k,n-1}) \quad (48)$$

The following assumption is extended from the convex case, and it is common for non-convex environments [31], [32], [38]. It assumes that the variance of the gradient noise is bounded by a term associated with $\mathbf{w}_{k,n-1}$. This assumption is weaker than the one where the term is bounded by a constant [27], [33].

Assumption 6. (Moments of gradient noise) For each agent

k , the gradient noise satisfies

$$\mathbb{E} \left\{ \|\bar{\mathbf{s}}_{k,n}(\mathbf{w}_{k,n-1})\|^2 \mid \mathcal{F}_{n-1} \right\} \leq \beta^2 \|\overline{\nabla_w J_k}(\mathbf{w}_{k,n-1})\|^2 + \sigma^2 \quad (49)$$

for some non-negative scalars β and σ . \square

Now consider the weighted average of the weight iterates at all agents defined by

$$\mathbf{w}_{c,n} \triangleq \sum_{k=1}^K \pi_k \mathbf{w}_{k,n} \quad (50)$$

and introduce the following block vectors:

$$\mathbf{w}_n \triangleq \text{col}\{\mathbf{w}_{k,n}\}_{k=1}^K \quad (51)$$

$$\mathbf{w}_{c,n} \triangleq \mathbb{1}_K \otimes \mathbf{w}_{c,n} \quad (52)$$

$$\mathcal{G}_{n-1} \triangleq \text{col}\{\overline{\nabla_w J_k}(\mathbf{w}_{k,n-1})\} \quad (53)$$

$$\bar{\mathbf{s}}_n^B \triangleq \text{col}\{\bar{\mathbf{s}}_{k,n}^B\} \quad (54)$$

Then, algorithm (43a)–(43c) can be rewritten as

$$\mathbf{w}_n = \mathcal{A}^\top (\mathbf{w}_{n-1} - \mu \mathcal{G}_{n-1} - \mu \bar{\mathbf{s}}_n^B) \quad (55)$$

We then have the next statements to measure the difference between \mathbf{w}_n and $\mathbf{w}_{c,n}$. The associated proofs can be found in Appendix D.

Lemma 3. (Network disagreement) *Under Assumptions 1–2 and 5–6, and with sufficiently small step size μ , the mean-square disagreement between \mathbf{w}_n and $\mathbf{w}_{c,n}$ can be bounded after enough iterations n_0 , namely, it holds that:*

$$\mathbb{E} \|\mathbf{w}_n - \mathbf{w}_{c,n}\|^2 \leq O(\mu^2) \quad (56)$$

for

$$n \geq n_0 \geq O\left(\frac{\log \mu}{\log t}\right) \quad (57)$$

where $t = \|\mathcal{J}_\alpha^\top\| < 1$. \square

The above result extends Lemma 1 from [31], [32], [38], which studies the unperturbed environment without adversarial observations. Result (56) means that $\mathbf{w}_{k,n}$ will cluster around the centroid $\mathbf{w}_{c,n}$ after sufficient iterations, and the bounded perturbations do not ruin this property. Thus, the evolution of $\mathbf{w}_{k,n}$ can be well-described by the centroid $\mathbf{w}_{c,n}$, which allows us to use $\mathbf{w}_{c,n}$ as a proxy to examine the dynamics of all agents across the network.

In order to progress further with the network analysis in the non-convex environment, we write down the following recursion for the centroid:

$$\begin{aligned} \mathbf{w}_{c,n} &= \sum_{k=1}^K \pi_k \mathbf{w}_{k,n} = (\pi^\top \otimes I_M) \mathbf{w}_n \\ &= (\pi^\top \otimes I_M) \mathcal{A}^\top (\mathbf{w}_{n-1} - \mu \mathcal{G}_{n-1} - \mu \bar{\mathbf{s}}_n^B) \\ &\stackrel{(a)}{=} (\pi^\top \otimes I_M) \mathbf{w}_{n-1} - \mu (\pi^\top \otimes I_M) (\mathcal{G}_{n-1} + \bar{\mathbf{s}}_n^B) \end{aligned}$$

$$= \mathbf{w}_{c,n-1} - \mu \sum_{k=1}^K \pi_k \overline{\nabla_w J_k}(\mathbf{w}_{k,n-1}) - \mu \sum_{k=1}^K \pi_k \bar{\mathbf{s}}_{k,n}^B \quad (58)$$

where (a) follows from (7). We can rework this recursion by using $\mathbf{w}_{c,n-1}$ as the argument for $\overline{\nabla_w J_k}(\cdot)$ instead of $\mathbf{w}_{k,n-1}$:

$$\overline{\nabla_w J_k}(\mathbf{w}_{c,n-1}) \triangleq \mathbb{E}\{\nabla_w Q_k(\mathbf{w}_{c,n-1}; \hat{\mathbf{x}}_{k,n}, \mathbf{y}_{k,n})\} \quad (59)$$

where

$$\hat{\mathbf{x}}_{k,n} = \mathbf{x}_{k,n} + \hat{\boldsymbol{\delta}}_{k,n}(\mathbf{w}_{k,n-1}) \quad (60)$$

Observe that the gradient of $Q_k(\cdot)$ is evaluated at $\mathbf{w}_{c,n-1}$ in (59), while the term $\mathbf{w}_{k,n-1}$ is used in (60) to emphasize that the perturbation $\hat{\boldsymbol{\delta}}_{k,n}$ is still computed from $\mathbf{w}_{k,n-1}$ using (40). In this way, we can rewrite (58) in the form

$$\mathbf{w}_{c,n} = \mathbf{w}_{c,n-1} - \mu \sum_k \pi_k \overline{\nabla_w J_k}(\mathbf{w}_{c,n-1}) - \mu \mathbf{d}_{n-1} - \mu \hat{\mathbf{s}}_n^B \quad (61)$$

where we are introducing

$$\mathbf{d}_{n-1} \triangleq \sum_{k=1}^K \pi_k \left(\overline{\nabla_w J_k}(\mathbf{w}_{k,n-1}) - \overline{\nabla_w J_k}(\mathbf{w}_{c,n-1}) \right) \quad (62)$$

$$\hat{\mathbf{s}}_n^B \triangleq \sum_{k=1}^K \pi_k \bar{\mathbf{s}}_{k,n}^B \quad (63)$$

The vector \mathbf{d}_{n-1} arises from the disagreement between \mathbf{w}_{n-1} and the centroid $\mathbf{w}_{c,n-1}$, while $\hat{\mathbf{s}}_n^B$ aggregates the gradient noise across the network. It can be verified that the two error terms \mathbf{d}_{n-1} and $\hat{\mathbf{s}}_n^B$ are bounded in the mean-square sense, using Assumption 6 and Lemma 3. The proof can be found in Appendix E.

Lemma 4. (Error bounds) *Under Assumptions 1–2 and 5–6, and with sufficiently small step size μ , the two error terms $\hat{\mathbf{s}}_n^B$ and \mathbf{d}_{n-1} are bounded in the mean-square sense, namely, it holds that*

$$\mathbb{E} \|\hat{\mathbf{s}}_n^B\|^2 \leq \frac{1}{B} (\beta^2 G^2 + \sigma^2) \quad (64)$$

$$\mathbb{E} \|\mathbf{d}_{n-1}\|^2 \leq O(\mu^2) \quad (65)$$

\square

Since $J(w)$ defined by (1) is not guaranteed to be differentiable in the non-convex case, the convergence analysis of the adversarial diffusion strategy relies on the use of subgradients for $J(w)$. Basically, w° is a stationary point for $J(w)$ if $0 \in \partial J(w^\circ)$. If the subdifferential $\partial J(w)$ at w° does not contain the value zero but is close to it, then we say that w° is an approximate stationary point. Here we use the Moreau envelope method and L -weak convexity [30], [33], [34], [39], [40] to study near-stationarity for non-smooth loss functions¹.

¹A function $f(z)$ is said to be L -weakly convex if [30]:

$$f(z_2) \geq f(z_1) + \partial_z f(z_1)(z_2 - z_1) - \frac{L}{2} \|z_2 - z_1\|^2$$

It is also shown in [30] that L -weak convexity holds if $\nabla_z f(z)$ is L -Lipschitz.

Let $\epsilon = \max_k \{\epsilon_k\}$. The proof for the next theorem can be found in Appendix F.

Theorem 2. *Consider the adversarial diffusion strategy (43a)–(43c). Under Assumptions 1–2 and 5–6, and assuming $J(w)$ is lower bounded, the following inequality holds for N large enough:*

$$\|\widehat{w}_{N-1} - w_{c,N-1}\|^2 \leq \rho = O\left(\frac{1}{\mu N}\right) + O(\mu) + O(\epsilon^2) \quad (66)$$

where \widehat{w}_{N-1} is an approximate stationary point for $J(w)$ satisfying

$$\mathbb{E} \left\{ \min_{\zeta \in \partial_w J(\widehat{w}_{N-1})} \|\zeta\|^2 \right\} \leq \rho \quad (67)$$

which implies that the algorithm arrives at a point $w_{c,N-1}$ that is $O(\mu) + O(\epsilon^2)$ close to an approximate stationary point of $J(w)$ after enough iterations. \square

Theorem 2 is based on properties of the Moreau envelope, and it guarantees that when μ and ϵ are small, the adversarial diffusion algorithm (43a)–(43c) will converge to a point that is $O(\mu) + O(\epsilon^2)$ close to an approximate stationary point of $J(w)$. Furthermore, the term $O(\epsilon^2)$ in (67) arises from the approximation error of the inner maximization. When the maximizer can be found exactly, this term can be eliminated. As it is usually intractable to compute the accurate maximizer in the non-convex case, approximation methods are applied. Then, the smaller the ϵ is, the better the exact maximizer can be approximated by the Taylor expansion.

V. COMPUTER SIMULATIONS

A. Logistic regression

In this section, we illustrate the performance of the adversarial diffusion strategy from Algorithm 1 using a logistic regression application. Let γ be a binary variable that takes values from $\{-1, 1\}$, and let $\mathbf{h} \in \mathbb{R}^M$ be a feature variable. The robust logistic regression problem by a network of agents employs the risk functions:

$$J_k(w) = \mathbb{E} \max_{\|\delta\|_{p_k} \leq \epsilon_k} \left\{ \ln(1 + e^{-\gamma(\mathbf{h} + \delta)^\top w}) \right\} \quad (68)$$

Note that when $p_k = 2$, the analytical solution for the inner maximizer (i.e., the worst-case perturbation) is given by

$$\delta^* = -\epsilon_k \gamma \frac{w}{\|w\|} \quad (69)$$

which is consistent with the perturbation computed from FGM [7]. On the other hand, if $p_k = \infty$, the closed-form expression for the inner maximizer changes to

$$\delta^* = -\epsilon_k \gamma \text{sign}(w) \quad (70)$$

which is the perturbation computed from the FGSM method [15].

In our experiments, we use both the MNIST [41] and CIFAR10 [42] datasets, and randomly generate a graph with 20 nodes, shown in Fig. 1(a). For each dataset, three networks

are trained, including two homogeneous adversarial networks using ℓ_2 and ℓ_∞ bounded perturbations where all agents are attacked by the same type of perturbations, and one clean network trained with original clean samples. We limit our simulations to binary classification in this example. For this reason, we consider samples with digits 0 and 1 from MNIST, and images for airplanes and automobiles from CIFAR10. For the ℓ_2 case, we set the perturbation bound in (68) to $\epsilon_k = 4$ for MNIST and $\epsilon_k = 1.5$ for CIFAR10. In the same token, the attack strengths are set to $\epsilon_k = 0.3$ for MNIST and $\epsilon_k = 0.035$ for CIFAR10 under the ℓ_∞ setting. In the test phase, we compute the average classification error across the networks to measure the performance of the multi-agent system against perturbations of different strengths. In other words, we test the robustness of the trained networks in the worst situation where all agents receive adversarial examples.

We first illustrate the convergence of the algorithm, as anticipated by Theorem 1. From Fig. 2, we observe a steady decrease in the classification error towards a limiting value for each subplot.

The robust behavior of the algorithm to ℓ_2 and ℓ_∞ attacks is illustrated in Fig. 3 for both MNIST and CIFAR10. We comment on the curves for MNIST and similar remarks hold for CIFAR10. In the test phase, we use perturbations generated in one of two ways: using the worst-case (FGM for ℓ_2 and FGSM for ℓ_∞) construction and also using the DeepFool construction [43]. The red curve is obtained by training the network using the traditional diffusion learning strategy without accounting for robustness. The network is fed with worst-case perturbed samples (generated using FGM or FGSM) during testing corresponding to different levels of attack strength. The red curve shows that the classification error deteriorates rapidly. The blue curve repeats the same experiment except that the network is now trained with Algorithm 1. It is seen in the blue curve that the testing error is more resilient and the degradation is better controlled than the red curve. The same experiments are repeated using the same adversarially trained network and the clean one to show robustness to DeepFool attacks, where the perturbed samples are now generated using DeepFool as opposed to FGM or FGSM in the test phase. The purple curve shows the robustness of the clean network to DeepFool, while the green one corresponds to the adversarially trained network. Note that for ℓ_∞ attacks, i.e., Figs. 3(b) and 3(d), the DeepFool and FGSM possess similar destructive power so that the red and the purple curves, and also the blue and green curves, coincide with each other. Here robustness can be explained from two perspectives. First, the attack strength of DeepFool never outperforms the worst-case perturbations for the same model, so that robustness to the worst-case perturbation guarantees robustness to DeepFool. Second, comparing the purple and green curves, the evolution of the robustness of the networks to DeepFool is better controlled by our algorithm than the clean networks.

To further show the generalization ability of our algorithm, we test the robustness of the ℓ_2 -trained networks to a kind of heuristic noise called decision boundary attack (DBA) [44].

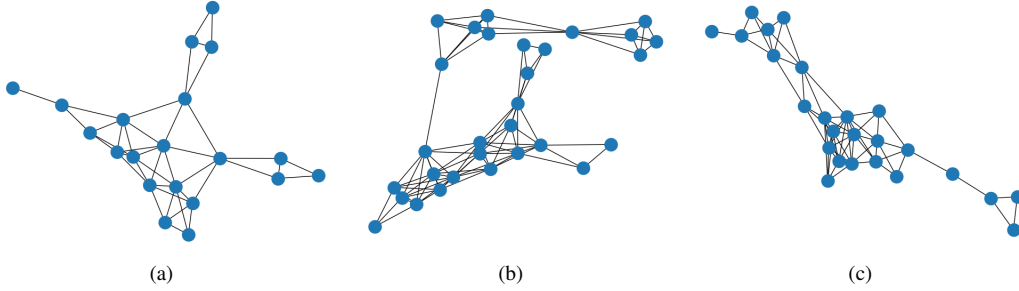


Fig. 1. The randomly generated graph structures used in the experiments. (a) Graph for convex scenario (MNIST and CIFAR10). (b) Graph for non-convex scenario (MNIST). (c) Graph for non-convex scenario (CIFAR10).

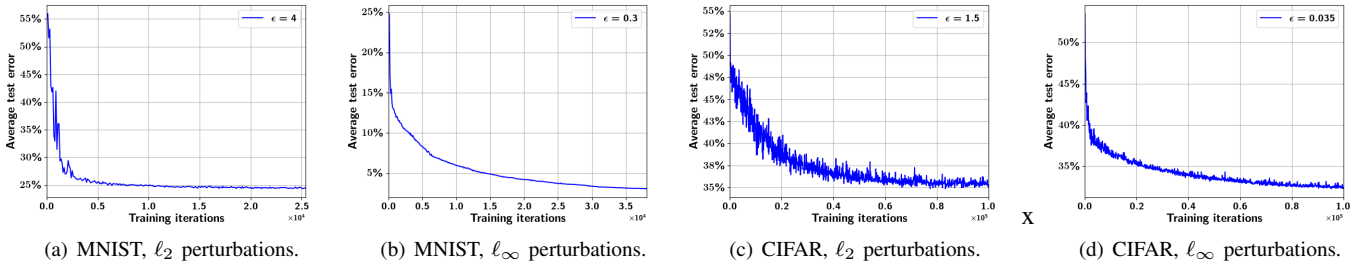


Fig. 2. Convergence plots for the two datasets using the logistic loss. The legends show the perturbation bounds used in the training phase. (a) The evolution of the average classification error across all agents over ℓ_2 adversarial examples bounded by $\epsilon_k = 4$ during training for MNIST. (b)–(d) follow a similar logic but for different norms and datasets.

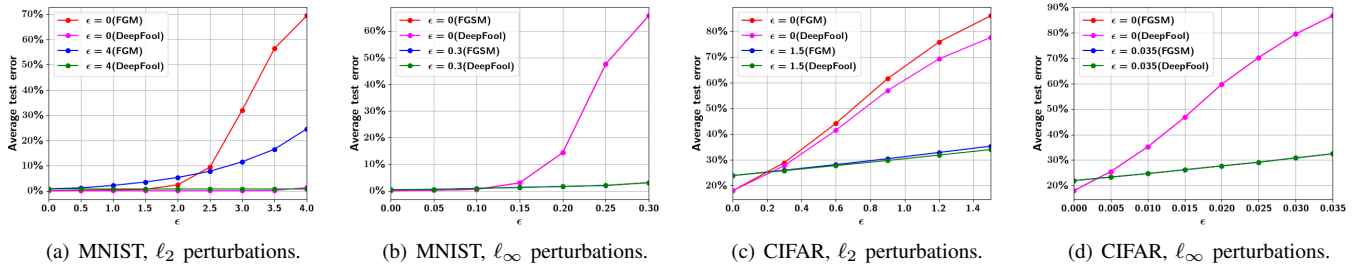


Fig. 3. Robustness plots for the two datasets in convex environments. (a) Average classification error over the graph versus perturbation size for MNIST to ℓ_2 attacks. The legends demonstrate the perturbation bound used in the training phase and the attack method in the test phase. For instance, $\epsilon = 0$ (FGM) corresponds to robustness of the clean network to FGM attack. (b)–(d) follow the similar logic but for different norms and datasets.

The associated results are shown in Table I, from which we observe that the robustness of the adversarially trained networks is better than their clean counterparts.

TABLE I

THE CLASSIFICATION ERROR OF THE ℓ_2 TRAINED NETWORKS UNDER DBA.

	clean	adv
MNIST	53.61%	4.12%
CIFAR10	40.76%	27.43%

In Fig. 4, we plot some randomly selected CIFAR10 images,

their perturbed versions, and the classification decisions generated by the nonrobust algorithm and its adversarial version listed in Algorithm 1. We observe from the figure that no matter which attack method is applied, the perturbations are always imperceptible to the human eye. Moreover, while the nonrobust algorithm fails to classify correctly in most cases, the adversarial algorithm is more robust and leads to fewer classification errors.

B. Neural networks

In this section, we illustrate the effectiveness of the adversarial diffusion strategy (43a)–(43c) in non-convex environments for the MNIST and CIFAR10 datasets for both homogeneous and heterogeneous networks. In the simulation, we utilize the random initialization technique from [37], which



Fig. 4. Visualization of the original and adversarial samples. The first row consists of 10 random original samples with the titles representing their true classes. The second row shows the adversarial examples generated by DeepFool and applied to a graph trained by the standard nonrobust algorithm. The third row shows the results obtained by the adversarial diffusion algorithm. The titles are the predictions by the corresponding models. The same construction is repeated in the last two rows using FGM. If the prediction of an image is wrong, the title is shown in red color. It is seen that the adversarial algorithm fails less frequently.

has been shown to enhance the stability of the adversarial training process in the single-agent case.

MNIST setup. For MNIST, we randomly generate a graph with 30 nodes for the distributed setting, and its structure is shown in Fig. 1(b), where each node corresponds to a convolutional neural network (CNN) model following a similar structure to the one used in [14] but adding the batch normalization [4], [45] layer. The output size of the last layer is 10. We set the perturbation bounds to $\epsilon_k = 2$ for ℓ_2 attacks and $\epsilon_k = 0.3$ for ℓ_∞ ones.

CIFAR10 setup. We use a randomly generated graph with 25 agents, where we now use the CNN structure from [46] for each agent. The graph structure is shown in Fig. 1(c). The perturbation bounds are set to $\epsilon_k = 0.5$ for ℓ_2 attacks and $\epsilon_k = 0.03$ for ℓ_∞ attacks. Note that as mentioned before, our algorithm is not restricted to the stochastic gradient optimizer. Since the CIFAR10 dataset is more complex than MNIST, the stochastic gradient momentum method [47] with cyclic learning rates [37] is applied to each agent.

1) *Homogeneous networks:* We show the results corresponding to the homogeneous networks, where all agents in the graph are attacked by the same type of perturbation (i.e., ϵ_k and p_k is uniform for all k). For instance, for MNIST with ℓ_2 attacks, all agents receive perturbations bounded by $\epsilon_k = 2$, and the global risk is

$$J(w) = \sum_{k=1}^{30} \pi_k \mathbb{E} \max_{\|\delta_k\| \leq 2} Q_k(w; \mathbf{x}_k + \delta_k, \mathbf{y}_k) \quad (71)$$

Fig. 5 shows the convergence plots for the two datasets, from which we observe that the average classification error across the networks to the trained attacks converges after sufficient iterations.

TABLE II

THE CLASSIFICATION ERROR FOR THE HOMOGENEOUS NETWORKS UNDER VARIOUS ATTACKS.

data	MNIST	MNIST	MNIST	MNIST	MNIST	MNIST
norm	ℓ_2	ℓ_2	ℓ_2	ℓ_∞	ℓ_∞	ℓ_∞
attack	PGM	DeepFool	FMN	PGD	DeepFool	FMN
error-clean	100%	100%	100%	100%	100%	100%
error-diff	21%	18%	24%	20%	14%	25%
error-nonco	33%	37%	40%	52%	34%	54%
error-centra	22%	22%	28%	24%	14%	25%

data	CIFAR	CIFAR	CIFAR	CIFAR	CIFAR	CIFAR
norm	ℓ_2	ℓ_2	ℓ_2	ℓ_∞	ℓ_∞	ℓ_∞
attack	PGM	DeepFool	FMN	PGD	DeepFool	FMN
error-clean	99%	98%	83%	100%	100%	100%
error-diff	32%	35%	34%	50%	49%	57%
error-nonco	63%	66%	66%	79%	82%	83%
error-centra	37%	39%	39%	57%	59%	63%

We next show how the robustness of the multi-agent systems can be improved by the proposed algorithm compared with the clean networks. Similar to the convex case, three networks are trained for each dataset, including two homogeneous networks adversarially trained by ℓ_2 and ℓ_∞ bounded perturbations respectively, and one clean system fed only with clean samples in the training phase, which is equivalent to the case of $\epsilon = 0$. Fig. 6 illustrates the robust behavior of the multi-agent systems to the attacks that are visible in the training process. That is, we observe from the red curve in each subplot a rapid increase for the average classification error across the network to adversarial examples. This demonstrates the vulnerability of the clean models. Fortunately, this phenomenon can be mitigated by the proposed algorithm as the blue curve shows. We further test the robustness of the networks to some multi-step attacks, i.e., PGD or PGM [14], DeepFool [43], and FMN [48], with the Foolbox package [49], and the results are shown in Table II, where the row *error-clean* corresponds to the classification error of the clean networks, and *error-diff* relates to the robustness of the adversarially trained networks by our diffusion algorithm. Different from the convex case where the closed-form solution for the inner maximization can be exactly obtained, it is only possible to find an approximation for it in the non-convex case. Thus, the FGM and FGSM attacks used in the training process are not the most powerful (i.e., worst-case) perturbations within the norm-bound regions.

We finally compare the robustness of the networks adversarially trained by three different distributed strategies: diffusion (i.e., our approach), non-cooperative, and centralized. Basically, all agents train their own models independently in the non-cooperative setting, while all agents share their data with a fusion center to do the computation in the centralized method. The results are shown in Fig. 7 and Table II, where the row *error-nonco* corresponds to the robustness of the

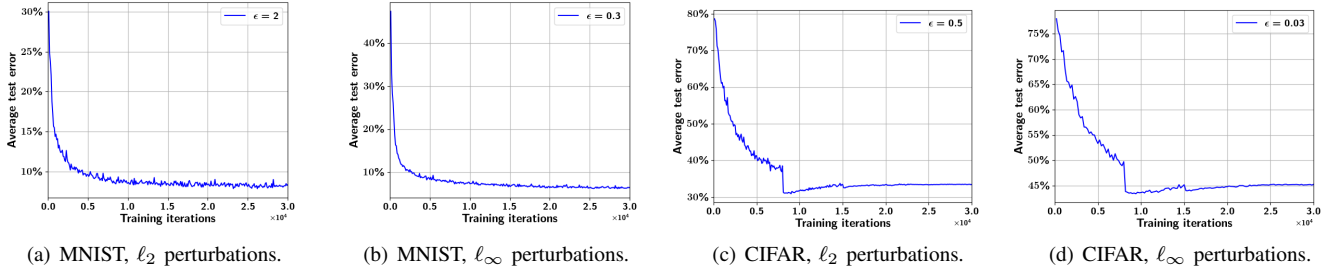


Fig. 5. Convergence plots for the two datasets in non-convex environments. The legends show the perturbation bound used in the training phase. (a) The evolution of the average classification error across all agents over ℓ_2 adversarial examples bounded by $\epsilon_k = 2$ during training for MNIST. (b)–(d) follow a similar logic but for different norms and datasets.

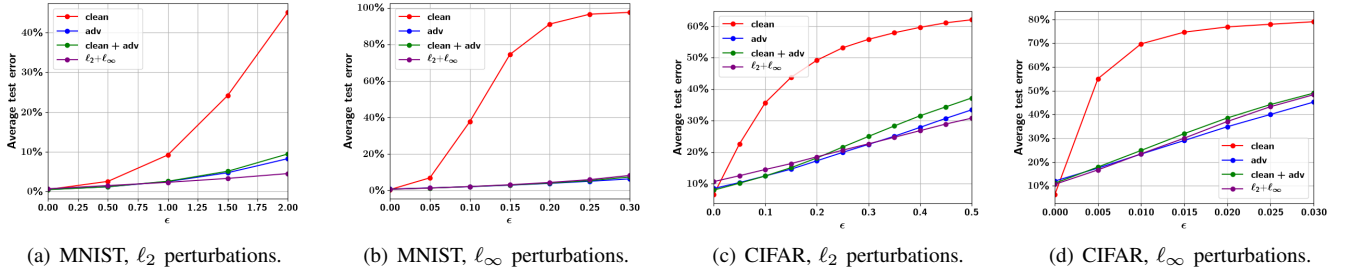


Fig. 6. Robustness plots for the two datasets in non-convex environments. The red, blue, green and purple curves in each subplot correspond to the robustness behaviour of the clean, homogeneous, clean+adv, and $\ell_2 + \ell_\infty$ heterogeneous networks respectively. (a) Average classification error across the networks versus perturbation size to FGM attack for MNIST. (b)–(d) follow a similar logic but for different norms and datasets.

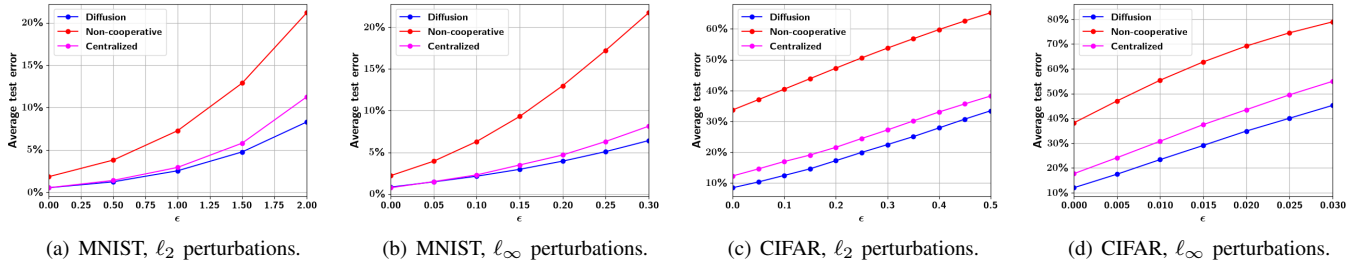


Fig. 7. Comparison among three distributed strategies: diffusion, non-cooperative, and centralized. (a) Classification error versus perturbation size for MNIST to FGM; (b)–(d) follow a similar logic but for different norms and datasets.

non-cooperative networks, and *error-centra* shows the results associated with the centralized method. Comparing the results associated with the three methods from Fig. 7 and Table II, we observe that the diffusion networks are more robust than the non-cooperative ones. This is due to the cooperation over the graph topology. Furthermore, we surprisingly observe that the robustness of the diffusion networks outperforms that of the centralized architectures, especially for the CIFAR10 dataset. This behavior is different from what one would observe under clean training [20], [38] and from the view that the decentralized method may hurt generalization [50]. One explanation for this phenomenon in the context of adversarial training is that decentralized stochastic gradient algorithms have been shown to favor more flat minimizers than the centralized method, and flat minimizers in turn have been shown to generalize better

than sharp minimizers [51]. To illustrate this effect, we plot the following empirical risk function:

$$\frac{1}{N} \sum_{i=1}^N Q(w; x_i + \hat{\delta}_i(w), y_i) \quad (72)$$

for choices of the form $w = \alpha w_d + (1 - \alpha)w_c$, where w_d corresponds to the centroid model obtained by our decentralized algorithm, and w_c is the centralized model. The result is shown in Fig. 8, from which we observe that the neighborhood of the centroid from the distributed solution is more flat than the sharp minima for the centralized solution. We also notice that the superiority of the diffusion method over the centralized solution is amplified in the context of adversarial training. For example, for CIFAR10, the clean accuracy of the diffusion

network is 1% higher than the centralized one in the clean training. However, this gap increases to 5% or even more (as Fig. 7 and Table II show) under adversarial training. This observation suggests that there is merit to networked learning where the graph topology contributes to robustness.

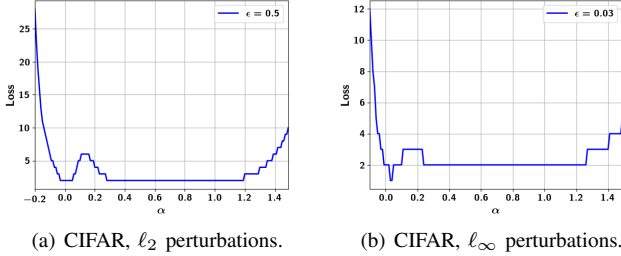


Fig. 8. The loss visualization for CIFAR10. The choice $\alpha = 0$ corresponds to the centralized model, while $\alpha = 1$ corresponds to the centroid model.

2) *Heterogeneous networks*: It is possible to consider situations where the perturbations at the agents are bounded by different norms p_k or attack strengths ϵ_k . This motivates us to study the robustness in heterogeneous settings. We simulate two kinds of heterogeneity in the experiment. In the first case, which is referred to *clean+adv*, half of the agents are trained adversarially while the other half is trained in the normal manner with clean samples. In the second type of heterogeneous networks, which are referred to l_2+l_∞ , half of the agents receive attacks generated from the l_2 norm, while the other half are attacked by l_∞ perturbations.

To train both heterogeneous networks, we repeat the procedure from training the homogeneous networks except that the upper bounds ϵ_k or the l_{p_k} norms may vary over the graph. The convergence plots are shown in Fig. 9, where we show the evolution of the average classification error across all agents to the attacks seen in the training process.

The robustness of the heterogeneous networks are illustrated by Fig. 6 and Table III. The green curves in Fig. 6 show the robustness evolution of the clean+adv networks to the trained perturbations against different attack strength and the purple curves correspond to the l_2+l_∞ networks. Comparing the results of the clean+adv and traditional clean networks in Fig. 6, from Table II and Table III, it is obvious that the former systems perform better than the latter ones. Thus, due to cooperation across the networks, the adversarial agents help improve the robustness of clean agents in the clean+adv networks. Likewise, comparing the results between the homogeneous and clean+adv networks, we observe some improvement for the clean accuracy in the clean+adv networks while their robustness deteriorates since now only a half of the agents are trained adversarially. This observation is associated with the trade-off between clean accuracy and robustness [17], [52], which is still an open issue even in the single-agent case. Similarly, as for the performance of the l_2+l_∞ networks, we observe that this kind of heterogeneous networks are still more robust than the traditional clean ones. Moreover, their robustness to l_2 attacks are enhanced by the l_∞ agents. However,

their robustness to l_∞ agents decreases. This phenomenon relates to the trade-off among multiple perturbations [16], [53] in single-agent learning.

VI. CONCLUSION

In this paper, we proposed a diffusion defense mechanism for adversarial attacks over graphs. We analyzed the different convergence properties of the proposed framework for convex and non-convex losses. We further illustrated the behavior of the trained networks to perturbations generated by different attack methods, and illustrated the enhanced robust behavior. Future directions can be on the trade-off problems in heterogeneous networks, which add more flexibility to the system than traditional single-agent learning.

APPENDIX A PROOF OF LEMMA 1

Proof. Before proving the affine Lipschitz condition, we first note that the l_2 distance between any two possible perturbations $\delta_{k,1}$ and $\delta_{k,2}$ from the region $\|\delta\|_{p_k} \leq \epsilon_k$ can be bounded in view of the equivalence of vector norms. Specifically, for any two vector norms $\|\cdot\|_a$ and $\|\cdot\|_b$ defined over a finite-dimensional space, there exist real numbers $0 < c_1 \leq c_2$ such that for any $\delta \in \mathbb{R}^M$:

$$c_1 \|\delta\|_a \leq \|\delta\|_b \leq c_2 \|\delta\|_a \quad (73)$$

according to which we say that for any l_p norm, if $\|\delta\|_p$ is bounded by ϵ_k , then $\|\delta\|$ is bounded by $O(\epsilon_k)$. For example, when $p_k = 1$, we have

$$\|\delta_{k,2} - \delta_{k,1}\| \leq \|\delta_{k,2} - \delta_{k,1}\|_1 \leq 2\epsilon_k \quad (74)$$

and when $p_k = \infty$, we have

$$\|\delta_{k,2} - \delta_{k,1}\| \leq \sqrt{M} \|\delta_2 - \delta_1\|_\infty \leq 2\sqrt{M}\epsilon_k \quad (75)$$

Furthermore, consider the maximum perturbation bound across all agents and denote it by

$$\epsilon = \max_k \epsilon_k \quad (76)$$

Then, the l_2 distance between any two possible perturbations δ_k and δ_ℓ from the regions $\|\delta\|_{p_k} \leq \epsilon_k$ and $\|\delta\|_{p_\ell} \leq \epsilon_\ell$ can also be bounded even if $p_k \neq p_\ell$ and $\epsilon_k \neq \epsilon_\ell$. For example, if $p_k = \infty$ and $p_\ell = 2$, we have

$$\|\delta_k - \delta_\ell\| \leq \|\delta_k\| + \|\delta_\ell\| \leq \sqrt{M}\epsilon_k + \epsilon_\ell = O(\epsilon) \quad (77)$$

Thus, for later use, no matter which perturbation norm is used, we can assume for any agents k and ℓ that the Euclidean norm of the respective perturbations satisfy

$$\|\delta_{k,2} - \delta_{k,1}\| \leq O(\epsilon_k), \quad \|\delta_k - \delta_\ell\| \leq O(\epsilon) \quad (78)$$

Next, for any $w_1, w_2 \in \mathbb{R}^M$, consider the problems:

$$\delta_2^* = \operatorname{argmax}_{\|\delta\|_{p_k} \leq \epsilon_k} Q_k(w_2; \mathbf{x}_k + \delta, \mathbf{y}_k) \quad (79)$$

$$\delta_1^* = \operatorname{argmax}_{\|\delta\|_{p_k} \leq \epsilon_k} Q_k(w_1; \mathbf{x}_k + \delta, \mathbf{y}_k) \quad (80)$$

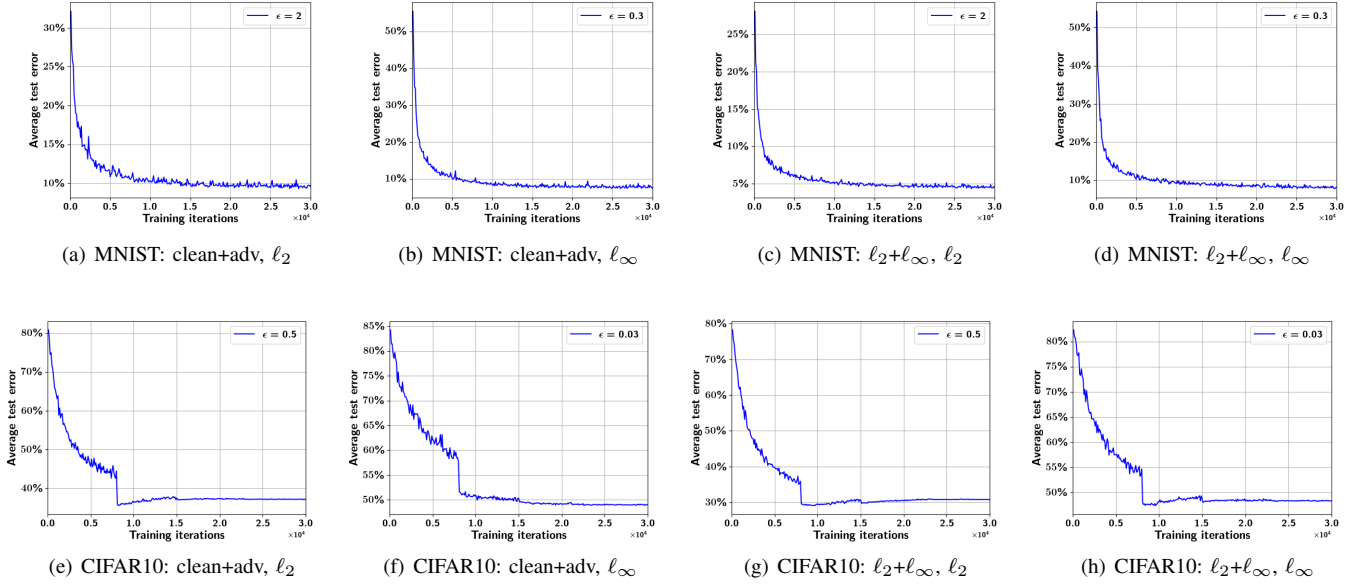


Fig. 9. Convergence plots for the two datasets in non-convex environments. (a) The evolution of the average classification error over l_2 adversarial examples bounded by $\epsilon_k = 2$ when training the clean+adv network associated with l_2 attacks for MNIST. (b) The evolution of the average classification error over l_∞ adversarial examples bounded by $\epsilon_k = 0.3$ when training the clean+adv network associated with l_∞ attacks for MNIST. (c) The evolution of the average classification error over l_2 adversarial examples bounded by $\epsilon_k = 2$ when training the l_2+l_∞ network for MNIST. (d) The evolution of the average classification error over l_∞ adversarial examples bounded by $\epsilon_k = 0.3$ when training the l_2+l_∞ network for MNIST. (e)–(h) follow a similar logic to (a)–(b) except now the dataset is CIFAR10.

TABLE III
THE CLASSIFICATION ERROR OF HETEROGENEOUS NETWORKS TO VARIOUS ATTACKS.

dada	MNIST	MNIST	MNIST	MNIST	MNIST	MNIST						
attack	PGM	DeepFool	FMN	PGD	DeepFool	FMN	PGM	DeepFool	FMN	PGD	DeepFool	FMN
model	clean+adv	clean+adv	clean+adv	clean+adv	clean+adv	clean+adv	l_2+l_∞	l_2+l_∞	l_2+l_∞	l_2+l_∞	l_2+l_∞	l_2+l_∞
ϵ	2	2	2	0.3	0.3	0.3	2	2	2	0.3	0.3	0.3
error	24%	22%	29%	54%	22%	54%	14%	13%	17%	55%	22%	52%
dada	CIFAR	CIFAR	CIFAR	CIFAR	CIFAR	CIFAR						
attack	PGM	DeepFool	FMN	PGD	DeepFool	FMN	PGM	DeepFool	FMN	PGD	DeepFool	FMN
model	clean+adv	clean+adv	clean+adv	clean+adv	clean+adv	clean+adv	l_2+l_∞	l_2+l_∞	l_2+l_∞	l_2+l_∞	l_2+l_∞	l_2+l_∞
ϵ	0.5	0.5	0.5	0.03	0.03	0.03	0.5	0.5	0.5	0.03	0.03	0.03
error	37%	38%	37%	57%	53%	67%	31%	33%	31%	52%	53%	63%

we then have:

$$\begin{aligned}
& \|\nabla_w Q_k(w_2; \mathbf{x}_k + \delta_2^*, \mathbf{y}_k) - \nabla_w Q_k(w_1; \mathbf{x}_k + \delta_1^*, \mathbf{y}_k)\| \\
&= \|\nabla_w Q_k(w_2; \mathbf{x}_k + \delta_2^*, \mathbf{y}_k) - \nabla_w Q_k(w_1; \mathbf{x}_k + \delta_2^*, \mathbf{y}_k) \\
&\quad + \nabla_w Q_k(w_1; \mathbf{x}_k + \delta_2^*, \mathbf{y}_k) - \nabla_w Q_k(w_1; \mathbf{x}_k + \delta_1^*, \mathbf{y}_k)\| \\
&\leq \|\nabla_w Q_k(w_2; \mathbf{x}_k + \delta_2^*, \mathbf{y}_k) - \nabla_w Q_k(w_1; \mathbf{x}_k + \delta_2^*, \mathbf{y}_k)\| \\
&\quad + \|\nabla_w Q_k(w_1; \mathbf{x}_k + \delta_2^*, \mathbf{y}_k) - \nabla_w Q_k(w_1; \mathbf{x}_k + \delta_1^*, \mathbf{y}_k)\| \\
&\stackrel{(a)}{\leq} L\|w_2 - w_1\| + L\|\delta_2^* - \delta_1^*\| \\
&\leq L\|w_2 - w_1\| + O(\epsilon_k) \tag{81}
\end{aligned}$$

where (a) follows from (8a) and (9a). Then, exchanging the expectation and differentiation operations (as permitted by the dominated convergence theorem in our cases of interest [4])

we get

$$\begin{aligned}
& \|\nabla_w J_k(w_2) - \nabla_w J_k(w_1)\|^2 \\
&\stackrel{(a)}{=} \|\nabla_w \mathbb{E} Q_k(w_2; \mathbf{x}_k + \delta_2^*, \mathbf{y}_k) - \nabla_w \mathbb{E} Q_k(w_1; \mathbf{x}_k + \delta_1^*, \mathbf{y}_k)\|^2 \\
&\leq \mathbb{E} \|\nabla_w Q_k(w_2; \mathbf{x}_k + \delta_2^*, \mathbf{y}_k) - \nabla_w Q_k(w_1; \mathbf{x}_k + \delta_1^*, \mathbf{y}_k)\|^2 \\
&\stackrel{(b)}{\leq} 2L^2\|w_2 - w_1\|^2 + O(\epsilon_k^2) \tag{82}
\end{aligned}$$

where (a) follows from (5), and (b) follows from (81) and Jensen's inequality:

$$\|x + y\|^2 \leq 2\|x\|^2 + 2\|y\|^2 \tag{83}$$

□

APPENDIX B
PROOF OF LEMMA 2

Proof. We first verify that the gradient noise has zero mean. Thus, note that

$$\begin{aligned} & \mathbb{E} \{ \mathbf{s}_{k,n} | \mathcal{F}_{n-1} \} \\ &= \mathbb{E} \{ \nabla_w Q_k(\mathbf{w}_{k,n-1}; \mathbf{x}_{k,n}^*, \mathbf{y}_{k,n}) - \nabla_w J_k(\mathbf{w}_{k,n-1}) | \mathcal{F}_{n-1} \} \\ &= \mathbb{E} \{ \nabla_w Q_k(\mathbf{w}_{k,n-1}; \mathbf{x}_{k,n}^*, \mathbf{y}_{k,n}) | \mathcal{F}_{n-1} \} \\ &\quad - \{ \nabla_w \mathbb{E} Q_k(\mathbf{w}_{k,n-1}; \mathbf{x}_{k,n}^*, \mathbf{y}_{k,n}) | \mathcal{F}_{n-1} \} \\ &= 0 \end{aligned} \quad (84)$$

Then, for the mini-batch gradient noise, we have

$$\begin{aligned} & \mathbb{E} \{ \mathbf{s}_{k,n}^B | \mathcal{F}_{n-1} \} \\ &= \mathbb{E} \left\{ \frac{1}{B} \sum_{b=1}^B \nabla_w Q_k(\mathbf{w}_{k,n-1}; \mathbf{x}_{k,n}^{b,*}, \mathbf{y}_{k,n}^b) \right. \\ &\quad \left. - \nabla_w J_k(\mathbf{w}_{k,n-1}) \middle| \mathcal{F}_{n-1} \right\} \\ &= \frac{1}{B} \sum_{b=1}^B \mathbb{E} \{ \mathbf{s}_{k,n} | \mathcal{F}_{n-1} \} = 0 \end{aligned} \quad (85)$$

Next we assess the variance of the gradient noise:

$$\begin{aligned} & \mathbb{E} \{ \|\mathbf{s}_{k,n}\|^2 | \mathcal{F}_{n-1} \} \\ &= \mathbb{E} \{ \|\nabla_w Q_k(\mathbf{w}_{k,n-1}; \mathbf{x}_{k,n}^*, \mathbf{y}_{k,n}) \\ &\quad - \nabla_w J_k(\mathbf{w}_{k,n-1})\|^2 | \mathcal{F}_{n-1} \} \\ &= \mathbb{E} \{ \|\nabla_w Q_k(\mathbf{w}_{k,n-1}; \mathbf{x}_{k,n}^*, \mathbf{y}_{k,n}) \\ &\quad - \nabla_w Q_k(w^*; \mathbf{x}_{k,n} + \delta_k^*(w^*), \mathbf{y}_{k,n}) \\ &\quad + \nabla_w Q_k(w^*; \mathbf{x}_{k,n} + \delta_k^*(w^*), \mathbf{y}_{k,n}) - \nabla_w J_k(\mathbf{w}_{k,n-1})\|^2 \\ &\stackrel{(a)}{\leq} 4\mathbb{E} \{ \|\nabla_w Q_k(\mathbf{w}_{k,n-1}; \mathbf{x}_{k,n}^*, \mathbf{y}_{k,n}) \\ &\quad - \nabla_w Q_k(w^*; \mathbf{x}_{k,n} + \delta_k^*(w^*), \mathbf{y}_{k,n})\|^2 \\ &\quad + 4\mathbb{E} \{ \|\nabla_w Q_k(w^*; \mathbf{x}_{k,n} + \delta_k^*(w^*), \mathbf{y}_{k,n})\|^2 \\ &\quad + 4\mathbb{E} \{ \|\nabla_w J_k(\mathbf{w}_{k,n-1}) - \nabla_w J_k(w^*)\|^2 + 4\|\nabla_w J_k(w^*)\|^2 \} \end{aligned} \quad (86)$$

where (a) follows from (83), $\mathbf{x}_{k,n}^*$ follows from (6) in which $\delta_{k,n}^*$ is the maximizer associated with $\mathbf{w}_{k,n-1}$, and

$$\delta_k^*(w^*) = \underset{\|\delta\|_{p_k} \leq \epsilon_k}{\operatorname{argmax}} Q_k(w^*; \mathbf{x}_{k,n} + \delta, \mathbf{y}_{k,n}) \quad (87)$$

is the maximizer corresponding to the global minimizer w^* . Note that

$$\nabla_w J_k(\mathbf{w}_{k,n-1}) = \mathbb{E} \nabla_w Q_k(\mathbf{w}_{k,n-1}; \mathbf{x}_{k,n}^*, \mathbf{y}_{k,n}) \quad (88)$$

$$\nabla_w J_k(w^*) = \mathbb{E} \nabla_w Q_k(w^*; \mathbf{x}_{k,n} + \delta_k^*(w^*), \mathbf{y}_{k,n}) \quad (89)$$

and from Jensen's inequality, we have

$$\|\mathbb{E} \mathbf{x}\|^2 \leq \mathbb{E} \|\mathbf{x}\|^2 \quad (90)$$

Substituting (88), (89) and (90) into (86), we obtain

$$\begin{aligned} & \mathbb{E} \{ \|\mathbf{s}_{k,n}\|^2 | \mathcal{F}_{n-1} \} \\ &\leq 8\mathbb{E} \{ \|\nabla_w Q_k(\mathbf{w}_{k,n-1}; \mathbf{x}_{k,n}^*, \mathbf{y}_{k,n}) \\ &\quad - \nabla_w Q_k(w^*; \mathbf{x}_{k,n} + \delta_k^*(w^*), \mathbf{y}_{k,n})\|^2 \\ &\quad + 8\mathbb{E} \{ \|\nabla_w Q_k(w^*; \mathbf{x}_{k,n} + \delta_k^*(w^*), \mathbf{y}_{k,n})\|^2 \\ &\stackrel{(a)}{\leq} 16L^2 \|\mathbf{w}_{k,n-1} - w^*\|^2 + O(\epsilon_k^2) \\ &\quad + 8\mathbb{E} \{ \|\nabla_w Q_k(w^*; \mathbf{x}_{k,n} + \delta_k^*(w^*), \mathbf{y}_{k,n})\|^2 \} \end{aligned} \quad (91)$$

where (a) follows from (81) and (83). Then for the mini-batch gradient noise, we have

$$\begin{aligned} & \mathbb{E} \{ \|\mathbf{s}_{k,n}^B\|^2 | \mathcal{F}_{n-1} \} \\ &= \mathbb{E} \left\{ \left\| \frac{1}{B} \sum_{b=1}^B \nabla_w Q_k(\mathbf{w}_{k,n-1}; \mathbf{x}_{k,n}^{b,*}, \mathbf{y}_{k,n}^{b,*}) \right. \right. \\ &\quad \left. \left. - \nabla_w J_k(\mathbf{w}_{k,n-1}) \right\|^2 \middle| \mathcal{F}_{n-1} \right\} \\ &\stackrel{(a)}{=} \frac{1}{B^2} \sum_{b=1}^B \mathbb{E} \{ \|\mathbf{s}_{k,n}\|^2 | \mathcal{F}_{n-1} \} \\ &\stackrel{(b)}{\leq} \frac{16L^2}{B} \|\mathbf{w}_{k,n-1} - w^*\|^2 + O(\epsilon_k^2) \\ &\quad + \frac{8}{B} \mathbb{E} \{ \|\nabla_w Q_k(w^*; \mathbf{x}_{k,n} + \delta_k^*(w^*), \mathbf{y}_{k,n})\|^2 \} \end{aligned} \quad (92)$$

where (a) is due to the fact that all data are sampled independently, and (b) follows from (91). \square

APPENDIX C
PROOF OF THEOREM 1

Proof. We first verify the convergence of $\mathbb{E} \|\check{\mathbf{w}}_n\|^2$. Conditioning both sides of (34) on \mathcal{F}_{n-1} , we obtain

$$\begin{aligned} & \mathbb{E} \{ \|\check{\mathbf{w}}_n\|^2 | \mathcal{F}_{n-1} \} \\ &= \mathbb{E} \left\{ \|\mathcal{J}_\alpha^\top \check{\mathbf{w}}_{n-1} + \mu \mathcal{J}_\alpha^\top \mathcal{V}_R^\top \nabla_w J(\mathbf{w}_{n-1}) \right. \\ &\quad \left. + \mu \mathcal{J}_\alpha^\top \mathcal{V}_R^\top \mathcal{S}_n^B \right\|^2 | \mathcal{F}_{n-1} \} \\ &\stackrel{(a)}{=} \|\mathcal{J}_\alpha^\top \check{\mathbf{w}}_{n-1} + \mu \mathcal{J}_\alpha^\top \mathcal{V}_R^\top \nabla_w J(\mathbf{w}_{n-1})\|^2 \\ &\quad + \mu^2 \mathbb{E} \{ \|\mathcal{J}_\alpha^\top \mathcal{V}_R^\top \mathcal{S}_n^B\|^2 | \mathcal{F}_{n-1} \} \\ &\stackrel{(b)}{\leq} t \|\check{\mathbf{w}}_{n-1}\|^2 + \frac{\mu^2 t^2}{1-t} \|\mathcal{V}_R^\top \nabla_w J(\mathbf{w}_{n-1})\|^2 \\ &\quad + \mu^2 t^2 \mathbb{E} \{ \|\mathcal{V}_R^\top \mathcal{S}_n^B\|^2 | \mathcal{F}_{n-1} \} \end{aligned} \quad (93)$$

where (a) follows from (16), and (b) from Jensen's inequality for any $t \in (0, 1)$. We select t as follows, and assume a small enough α such that (see [20, ch.9]):

$$t = \|\mathcal{J}_\alpha^\top\| = \sqrt{\tau(J_\alpha J_\alpha^\top)} = \lambda_2 + \alpha < 1 \quad (94)$$

Taking expectations of both sides, we have

$$\begin{aligned} \mathbb{E} \|\check{\mathbf{w}}_n\|^2 &\leq t \mathbb{E} \|\check{\mathbf{w}}_{n-1}\|^2 + \frac{\mu^2 t^2}{1-t} \mathbb{E} \|\mathcal{V}_R^\top \nabla_w J(\mathbf{w}_{n-1})\|^2 \\ &\quad + \mu^2 t^2 \mathbb{E} \|\mathcal{V}_R^\top \mathcal{S}_n^B\|^2 \end{aligned} \quad (95)$$

We now examine terms on the right-hand side of (95) one by one. First, with (31c), we have

$$\begin{aligned}
& \|\mathcal{V}_R^\top \nabla_w J(\mathbf{w}_{n-1})\|^2 \\
&= \|\mathcal{V}_R^\top \nabla_w J(\mathbf{w}_{n-1}) - \mathcal{V}_R^\top (\mathbb{1}\pi^\top \otimes I_M) \nabla_w J(\mathbf{w}_{n-1})\|^2 \\
&\stackrel{(a)}{\leq} \|\mathcal{V}_R^\top\|^2 \left(\sum_{k=1}^K \left\| \nabla_w J_k(\mathbf{w}_{k,n-1}) - \sum_{\ell=1}^K \pi_\ell \nabla_w J_\ell(\mathbf{w}_{\ell,n-1}) \right\|^2 \right) \\
&= \|\mathcal{V}_R^\top\|^2 \left(\sum_{k=1}^K \left\| \sum_{\ell=1}^K \pi_\ell (\nabla_w J_k(\mathbf{w}_{k,n-1}) - \nabla_w J_\ell(\mathbf{w}_{\ell,n-1})) \right\|^2 \right) \\
&\stackrel{(b)}{\leq} \|\mathcal{V}_R^\top\|^2 \left(\sum_{k=1}^K \sum_{\ell=1}^K \pi_\ell \|\nabla_w J_k(\mathbf{w}_{k,n-1}) - \nabla_w J_\ell(\mathbf{w}_{\ell,n-1})\|^2 \right) \tag{96}
\end{aligned}$$

where (a) follows from the triangle inequality of norms, and (b) follows from Jensen's inequality. To proceed, the gradient disagreement between any two agents can be bounded as follows:

$$\begin{aligned}
& \|\nabla_w J_k(\mathbf{w}_{k,n-1}) - \nabla_w J_\ell(\mathbf{w}_{\ell,n-1})\|^2 \\
&= \|\nabla_w J_k(\mathbf{w}_{k,n-1}) - \nabla_w J_k(\mathbf{w}_{\ell,n-1}) + \nabla_w J_k(\mathbf{w}_{\ell,n-1}) \\
&\quad - \nabla_w J_\ell(\mathbf{w}_{\ell,n-1})\|^2 \\
&\leq 2 \|\nabla_w J_k(\mathbf{w}_{k,n-1}) - \nabla_w J_k(\mathbf{w}_{\ell,n-1})\|^2 \\
&\quad + 2 \|\nabla_w J_k(\mathbf{w}_{\ell,n-1}) - \nabla_w J_\ell(\mathbf{w}_{\ell,n-1})\|^2 \\
&\stackrel{(a)}{\leq} 4L^2 \|\mathbf{w}_{k,n-1} - \mathbf{w}_{\ell,n-1}\|^2 + c^2 \\
&\leq 8L^2 \|\tilde{\mathbf{w}}_{k,n-1} - \bar{\mathbf{w}}_{n-1}\|^2 + 8L^2 \|\tilde{\mathbf{w}}_{\ell,n-1} - \bar{\mathbf{w}}_{n-1}\|^2 + c^2 \tag{97}
\end{aligned}$$

where (a) follows from Lemma 1 and the following inequality in which the constant c is defined and the non-iid data over space is considered:

$$\begin{aligned}
& \|\nabla_w J_k(\mathbf{w}_{\ell,n-1}) - \nabla_w J_\ell(\mathbf{w}_{\ell,n-1})\|^2 \\
&\leq \mathbb{E} \|\nabla_w Q_k(\mathbf{w}_{\ell,n-1}; \mathbf{x}_k + \delta_k^*, \mathbf{y}_k) \\
&\quad - \nabla_w Q_\ell(\mathbf{w}_{\ell,n-1}; \mathbf{x}_\ell + \delta_\ell^*, \mathbf{y}_\ell)\|^2 \\
&\leq \mathbb{E} \|\nabla_w Q_k(\mathbf{w}_{\ell,n-1}; \mathbf{x}_k + \delta_k^*, \mathbf{y}_k) \\
&\quad - \nabla_w Q_k(\mathbf{w}_{\ell,n-1}; \mathbf{x}_\ell + \delta_\ell^*, \mathbf{y}_k) \\
&\quad + \nabla_w Q_k(\mathbf{w}_{\ell,n-1}; \mathbf{x}_\ell + \delta_\ell^*, \mathbf{y}_k) \\
&\quad - \nabla_w Q_k(\mathbf{w}_{\ell,n-1}; \mathbf{x}_\ell + \delta_\ell^*, \mathbf{y}_\ell) \\
&\quad + \nabla_w Q_k(\mathbf{w}_{\ell,n-1}; \mathbf{x}_\ell + \delta_\ell^*, \mathbf{y}_\ell) \\
&\quad - \nabla_w Q_\ell(\mathbf{w}_{\ell,n-1}; \mathbf{x}_\ell + \delta_\ell^*, \mathbf{y}_\ell)\|^2 \\
&\stackrel{(a)}{\leq} 6L^2 \mathbb{E} \|\mathbf{x}_k - \mathbf{x}_\ell\|^2 + 6L^2 \mathbb{E} \|\delta_k - \delta_\ell\|^2 + 3L^2 \mathbb{E} \|\mathbf{y}_k - \mathbf{y}_\ell\|^2 \\
&\quad + 3C^2 \\
&\stackrel{(b)}{\leq} O(\epsilon^2) + 3C^2 + 6L^2 \mathbb{E} \|\mathbf{x}_k - \mathbf{x}_\ell\|^2 + 3L^2 \mathbb{E} \|\mathbf{y}_k - \mathbf{y}_\ell\|^2 \triangleq c^2 \tag{98}
\end{aligned}$$

where (a) follows from the Lipschitz conditions in Assumptions 1 and 4, (b) from (78), and δ_k^* and δ_ℓ^* are maximizers

associated with agents k and ℓ respectively, namely,

$$\delta_k^* = \operatorname{argmax}_{\|\delta\|_{p_k} \leq \epsilon_k} Q_k(\mathbf{w}_{\ell,n-1}; \mathbf{x}_k + \delta, \mathbf{y}_k) \tag{99}$$

$$\delta_\ell^* = \operatorname{argmax}_{\|\delta\|_{p_\ell} \leq \epsilon_\ell} Q_\ell(\mathbf{w}_{\ell,n-1}; \mathbf{x}_\ell + \delta, \mathbf{y}_\ell) \tag{100}$$

Substituting (97) into (96), we get

$$\begin{aligned}
& \|\mathcal{V}_R^\top \nabla_w J(\mathbf{w}_{n-1})\|^2 \\
&\leq \|\mathcal{V}_R^\top\|^2 \left(\sum_{k=1}^K \sum_{\ell=1}^K \pi_\ell \left(8L^2 \|\tilde{\mathbf{w}}_{k,n-1} - \bar{\mathbf{w}}_{n-1}\|^2 \right. \right. \\
&\quad \left. \left. + 8L^2 \|\tilde{\mathbf{w}}_{\ell,n-1} - \bar{\mathbf{w}}_{n-1}\|^2 + c^2 \right) \right) \\
&= \|\mathcal{V}_R^\top\|^2 \left(8L^2 \sum_k \|\tilde{\mathbf{w}}_{k,n-1} - \bar{\mathbf{w}}_{n-1}\|^2 + \right. \\
&\quad \left. 8KL^2 \sum_\ell \pi_\ell \|\tilde{\mathbf{w}}_{\ell,n-1} - \bar{\mathbf{w}}_{n-1}\|^2 + Kc^2 \right) \\
&\stackrel{(a)}{\leq} \|\mathcal{V}_R^\top\|^2 \|\mathcal{V}_L\|^2 (8L^2 + 8KL^2) \|\check{\mathbf{w}}_{n-1}\|^2 + \|\mathcal{V}_R^\top\|^2 Kc^2 \tag{101}
\end{aligned}$$

where in (a) we utilize (31a) and introduce the block vector $\check{\mathbf{w}}_{n-1} = \operatorname{col}\{\bar{\mathbf{w}}_{n-1}\}_{k=1}^K$ to note that:

$$\begin{aligned}
& \sum_k \|\tilde{\mathbf{w}}_{k,n-1} - \bar{\mathbf{w}}_{n-1}\|^2 \\
&= \|\check{\mathbf{w}}_{n-1} - \bar{\mathbf{w}}_{n-1}\|^2 = \|(I_{KM} - \mathbb{1}\pi^\top \otimes I_M) \check{\mathbf{w}}_{n-1}\|^2 \\
&= \|\mathcal{V}_L \mathcal{V}_R^\top \check{\mathbf{w}}_{n-1}\|^2 = \|\mathcal{V}_L \check{\mathbf{w}}_{n-1}\|^2 \tag{102}
\end{aligned}$$

Next, we bound $\mathcal{V}_R^\top \mathbf{s}_n^B$. By utilizing (31c) again, we have

$$\begin{aligned}
& \mathbb{E} \|\mathcal{V}_R^\top \mathbf{s}_n^B\|^2 \\
&= \mathbb{E} \|\mathcal{V}_R^\top \mathbf{s}_n^B - \mathcal{V}_R^\top (\mathbb{1}\pi^\top \otimes I_M) \mathbf{s}_n^B\|^2 \\
&\leq \|\mathcal{V}_R^\top\|^2 \left(\sum_k \sum_\ell \pi_\ell \mathbb{E} \|\mathbf{s}_{k,n}^B(\mathbf{w}_{k,n-1}) - \mathbf{s}_{\ell,n}^B(\mathbf{w}_{\ell,n-1})\|^2 \right) \\
&\stackrel{(a)}{\leq} (36KL^2 + 36L^2) \|\mathcal{V}_R^\top\|^2 \|\mathcal{V}_L\|^2 \mathbb{E} \|\check{\mathbf{w}}_{n-1}\|^2 + \|\mathcal{V}_R^\top\|^2 a^2 K \tag{103}
\end{aligned}$$

where (a) follows from (102) and the following inequality in which the constant a is defined:

$$\begin{aligned}
& \mathbb{E} \|\mathbf{s}_{k,n}^B(\mathbf{w}_{k,n-1}) - \mathbf{s}_{\ell,n}^B(\mathbf{w}_{\ell,n-1})\|^2 \\
&= \mathbb{E} \left\| \frac{1}{B} \sum_b \nabla_w Q_k(\mathbf{w}_{k,n-1}; \mathbf{x}_{k,n}^b + \delta_{k,n}^{b,*}, \mathbf{y}_{k,n}^b) \right. \\
&\quad \left. - \frac{1}{B} \sum_b \nabla_w Q_\ell(\mathbf{w}_{\ell,n-1}; \mathbf{x}_{\ell,n}^b + \delta_{\ell,n}^{b,*}, \mathbf{y}_{\ell,n}^b) \right. \\
&\quad \left. - \nabla_w J_k(\mathbf{w}_{k,n-1}) + \nabla_w J_\ell(\mathbf{w}_{\ell,n-1}) \right\|^2 \\
&\stackrel{(a)}{\leq} \frac{2}{B} \sum_b \mathbb{E} \|\nabla_w Q_k(\mathbf{w}_{k,n-1}; \mathbf{x}_{k,n}^b + \delta_{k,n}^{b,*}, \mathbf{y}_{k,n}^b) \\
&\quad - \nabla_w Q_\ell(\mathbf{w}_{\ell,n-1}; \mathbf{x}_{\ell,n}^b + \delta_{\ell,n}^{b,*}, \mathbf{y}_{\ell,n}^b)\|^2
\end{aligned}$$

$$\begin{aligned}
& + 2\mathbb{E} \|\nabla_w J_k(\mathbf{w}_{k,n-1}) - \nabla_w J_\ell(\mathbf{w}_{\ell,n-1})\|^2 \\
\leq & \frac{2}{B} \mathbb{E} \|\nabla_w Q_k(\mathbf{w}_{k,n-1}; \mathbf{x}_{k,n}^b + \delta_{k,n}^{b,*}, \mathbf{y}_{k,n}^b) \\
& - \nabla_w Q_k(\mathbf{w}_{k,n-1}; \mathbf{x}_{k,n}^b + \delta_{\ell,n}^{b,*}, \mathbf{y}_{k,n}^b) \\
& + \nabla_w Q_k(\mathbf{w}_{k,n-1}; \mathbf{x}_{k,n}^b + \delta_{\ell,n}^{b,*}, \mathbf{y}_{k,n}^b) \\
& - \nabla_w Q_k(\mathbf{w}_{\ell,n-1}; \mathbf{x}_{k,n}^b + \delta_{\ell,n}^{b,*}, \mathbf{y}_{k,n}^b) \\
& + \nabla_w Q_k(\mathbf{w}_{\ell,n-1}; \mathbf{x}_{k,n}^b + \delta_{\ell,n}^{b,*}, \mathbf{y}_{k,n}^b) \\
& - \nabla_w Q_\ell(\mathbf{w}_{\ell,n-1}; \mathbf{x}_{k,n}^b + \delta_{\ell,n}^{b,*}, \mathbf{y}_{k,n}^b) \\
& + \nabla_w Q_\ell(\mathbf{w}_{\ell,n-1}; \mathbf{x}_{k,n}^b + \delta_{\ell,n}^{b,*}, \mathbf{y}_{k,n}^b) \\
& - \nabla_w Q_\ell(\mathbf{w}_{\ell,n-1}; \mathbf{x}_{\ell,n}^b + \delta_{\ell,n}^{b,*}, \mathbf{y}_{k,n}^b) \\
& + \nabla_w Q_\ell(\mathbf{w}_{\ell,n-1}; \mathbf{x}_{\ell,n}^b + \delta_{\ell,n}^{b,*}, \mathbf{y}_{k,n}^b) \\
& - \nabla_w Q_\ell(\mathbf{w}_{\ell,n-1}; \mathbf{x}_{\ell,n}^b + \delta_{\ell,n}^{b,*}, \mathbf{y}_{\ell,n}^b)\|^2 \\
& + 2\mathbb{E} \|\nabla_w J_k(\mathbf{w}_{k,n-1}) - \nabla_w J_\ell(\mathbf{w}_{\ell,n-1})\|^2 \\
\stackrel{(b)}{\leq} & 10L^2 \mathbb{E} \|\delta_{k,n}^{b,*} - \delta_{\ell,n}^{b,*}\|^2 + 10L^2 \mathbb{E} \|\mathbf{w}_{k,n-1} - \mathbf{w}_{\ell,n-1}\|^2 \\
& + 10L^2 C^2 + 10L^2 \mathbb{E} \|\mathbf{x}_k - \mathbf{x}_\ell\|^2 + 10L^2 \mathbb{E} \|\mathbf{y}_k - \mathbf{y}_\ell\|^2 \\
& + 8L^2 \|\mathbf{w}_{k,n-1} - \mathbf{w}_{\ell,n-1}\|^2 + O(\epsilon^2) + 8C^2 \\
\leq & 18L^2 \mathbb{E} \|\mathbf{w}_{k,n-1} - \mathbf{w}_{\ell,n-1}\|^2 + a^2 \tag{104}
\end{aligned}$$

where (a) follows from (83), and (b) from (13), (97), Assumptions 2 and 4, and

$$\begin{aligned}
a^2 \triangleq & 10L^2 (\mathbb{E} \|\mathbf{x}_k - \mathbf{x}_\ell\|^2 + \mathbb{E} \|\mathbf{y}_k - \mathbf{y}_\ell\|^2) + C^2(10L^2 + 8) \\
& + O(\epsilon^2) \tag{105}
\end{aligned}$$

Now substituting (101) and (103) into (95), we get

$$\begin{aligned}
& \mathbb{E} \|\tilde{\mathbf{w}}_n\|^2 \\
\leq & t\mathbb{E} \|\tilde{\mathbf{w}}_{n-1}\|^2 + \frac{\mu^2 t^2}{1-t} \|\mathcal{V}_R^\top\|^2 \|\mathcal{V}_L\|^2 (8L^2 + 8KL^2) \mathbb{E} \|\tilde{\mathbf{w}}_{n-1}\|^2 \\
& + \mu^2 t^2 (36KL^2 + 36L^2) \|\mathcal{V}_R^\top\|^2 \|\mathcal{V}_L\|^2 \mathbb{E} \|\tilde{\mathbf{w}}_{n-1}\|^2 \\
& + \frac{\mu^2 t^2}{1-t} \|\mathcal{V}_R^\top\|^2 Kc^2 + \mu^2 t^2 \|\mathcal{V}_R^\top\|^2 a^2 K \\
= & (t + O(\mu^2)) \mathbb{E} \|\tilde{\mathbf{w}}_{n-1}\|^2 + O(\mu^2) \tag{106}
\end{aligned}$$

where $t + O(\mu^2) < 1$ when μ is sufficiently small. Then, iterating recursion (106) gives

$$\mathbb{E} \|\tilde{\mathbf{w}}_n\|^2 \leq (t + O(\mu^2))^{n+1} \mathbb{E} \|\tilde{\mathbf{w}}_{-1}\|^2 + O(\mu^2) \tag{107}$$

from which after enough iterations \tilde{n} with

$$\tilde{n} \geq O\left(\frac{\log \mu}{\log(t + O(\mu^2))}\right) \tag{108}$$

we get

$$\limsup_{n \rightarrow \infty} \mathbb{E} \|\tilde{\mathbf{w}}_n\|^2 \leq \mu^2 \tilde{c}_\epsilon^2 = O(\mu^2) \tag{109}$$

where

$$\tilde{c}_\epsilon^2 = \frac{2\|\mathcal{V}_R^\top\|^2 t^2}{1-t-O(\mu^2)} \left(\frac{Kc^2}{1-t} + a^2 K \right) \tag{110}$$

Next we examine the convergence of $\mathbb{E} \|\tilde{\mathbf{w}}_n\|^2$. Squaring

and taking expectations of (33) conditioned on \mathcal{F}_{n-1} , we have

$$\begin{aligned}
& \mathbb{E} \{ \|\tilde{\mathbf{w}}_n\|^2 | \mathcal{F}_{n-1} \} \\
\stackrel{(a)}{=} & \left\| \tilde{\mathbf{w}}_{n-1} + \mu \sum_k \pi_k \nabla_w J_k(\mathbf{w}_{k,n-1}) \right\|^2 \\
& + \mu^2 \mathbb{E} \left\{ \left\| \sum_k \pi_k \mathbf{s}_{k,n}^B(\mathbf{w}_{k,n-1}) \right\|^2 | \mathcal{F}_{n-1} \right\} \\
= & \|\tilde{\mathbf{w}}_{n-1}\|^2 + 2\mu \sum_k \pi_k \nabla_{w^\top} J_k(\mathbf{w}_{k,n-1}) \tilde{\mathbf{w}}_{n-1} \\
& + \mu^2 \left\| \sum_k \pi_k \nabla_w J_k(\mathbf{w}_{k,n-1}) \right\|^2 \\
& + \mu^2 \mathbb{E} \left\{ \left\| \sum_k \pi_k \mathbf{s}_{k,n}^B(\mathbf{w}_{k,n-1}) \right\|^2 | \mathcal{F}_{n-1} \right\} \tag{111}
\end{aligned}$$

where (a) follows from (16). We explore the right-hand terms of (111) one by one. First, for the term associated with the gradient noise, we have

$$\begin{aligned}
& \mathbb{E} \left\{ \left\| \sum_k \pi_k \mathbf{s}_{k,n}^B(\mathbf{w}_{k,n-1}) \right\|^2 | \mathcal{F}_{n-1} \right\} \\
\stackrel{(a)}{\leq} & \sum_k \pi_k \mathbb{E} \{ \|\mathbf{s}_{k,n}^B(\mathbf{w}_{k,n-1})\|^2 | \mathcal{F}_{n-1} \} \\
\stackrel{(b)}{\leq} & \beta_{\max}^2 \sum_k \pi_k \|\tilde{\mathbf{w}}_{k,n-1}\|^2 + \sigma^2 \tag{112}
\end{aligned}$$

where (a) follows from Jensen's inequality, (b) follows from (17), and

$$\beta_{\max}^2 = \max_k \{\beta_{k,\epsilon}^2\}, \quad \sigma^2 = \sum_k \pi_k \sigma_k^2 \tag{113}$$

Second, since w^* is the global minimizer, we have

$$\sum_k \pi_k \nabla_w J_k(w^*) = 0 \tag{114}$$

However, it is not guaranteed that $\nabla_w J_k(w^*) = 0$ since the local minimizers w_k^* and the global global minimizer w^* may be different. Thus, we have

$$\begin{aligned}
& \left\| \sum_k \pi_k \nabla_w J_k(\mathbf{w}_{k,n-1}) \right\|^2 \\
= & \left\| \sum_k \pi_k \nabla_w J_k(\mathbf{w}_{k,n-1}) - \sum_k \pi_k \nabla_w J_k(w^*) \right\|^2 \\
\stackrel{(a)}{\leq} & \sum_k \pi_k \|\nabla_w J_k(\mathbf{w}_{k,n-1}) - \nabla_w J_k(w^*)\|^2 \\
\stackrel{(b)}{\leq} & 2L^2 \sum_k \pi_k \|\tilde{\mathbf{w}}_{k,n-1}\|^2 + O(\epsilon^2) \tag{115}
\end{aligned}$$

where (a) follows from Jensen's inequality, and (b) follows from (13).

Next, taking expectations of the inner product term, and substituting (114) into it, we have

$$\begin{aligned} & \mathbb{E} \left\{ \sum_k \pi_k \nabla_{\mathbf{w}^\top} J_k(\mathbf{w}_{k,n-1}) \bar{\mathbf{w}}_{n-1} \right\} \\ &= \sum_k \pi_k \mathbb{E} (\nabla_{\mathbf{w}} J_k(\mathbf{w}_{k,n-1}) - \nabla_{\mathbf{w}} J_k(\mathbf{w}^*))^\top (\bar{\mathbf{w}}_{n-1} \\ & \quad - \tilde{\mathbf{w}}_{k,n-1} + \tilde{\mathbf{w}}_{k,n-1}) \end{aligned} \quad (116)$$

where since $J_k(\mathbf{w})$ is ν -strongly convex, we get

$$\mathbb{E} (\nabla_{\mathbf{w}} J_k(\mathbf{w}_{k,n-1}) - \nabla_{\mathbf{w}} J_k(\mathbf{w}^*))^\top \tilde{\mathbf{w}}_{k,n-1} \leq -\nu \mathbb{E} \|\tilde{\mathbf{w}}_{k,n-1}\|^2 \quad (117)$$

and

$$\begin{aligned} & \sum_k \pi_k \mathbb{E} (\nabla_{\mathbf{w}} J_k(\mathbf{w}_{k,n-1}) - \nabla_{\mathbf{w}} J_k(\mathbf{w}^*))^\top (\bar{\mathbf{w}}_{n-1} - \tilde{\mathbf{w}}_{k,n-1}) \\ & \stackrel{(a)}{\leq} \sum_k \pi_k \mathbb{E} \|\nabla_{\mathbf{w}} J_k(\mathbf{w}_{k,n-1}) - \nabla_{\mathbf{w}} J_k(\mathbf{w}^*)\| \|\bar{\mathbf{w}}_{n-1} - \tilde{\mathbf{w}}_{k,n-1}\| \\ & \stackrel{(b)}{\leq} \sum_k \pi_k \sqrt{\mathbb{E} \|\nabla_{\mathbf{w}} J_k(\mathbf{w}_{k,n-1}) - \nabla_{\mathbf{w}} J_k(\mathbf{w}^*)\|^2} \\ & \quad \times \sqrt{\mathbb{E} \|\bar{\mathbf{w}}_{n-1} - \tilde{\mathbf{w}}_{k,n-1}\|^2} \\ & \stackrel{(c)}{\leq} \sum_k \pi_k h \mu \sqrt{2L^2 \mathbb{E} \|\tilde{\mathbf{w}}_{k,n-1}\|^2 + O(\epsilon^2)} \\ & \stackrel{(d)}{\leq} h \mu L^2 \sum_k \pi_k \mathbb{E} \|\tilde{\mathbf{w}}_{k,n-1}\|^2 + h \mu \left(O(\epsilon^2) + \frac{1}{2} \right) \end{aligned} \quad (118)$$

where (a) and (b) follow from the Cauchy-Schwarz inequality, (c) follows from (13), (102) and (109), and $h \triangleq \|\mathcal{V}_L\| \check{c}_\epsilon$. That is, from (102) and (109), we know after enough iterations:

$$\begin{aligned} & \sqrt{\mathbb{E} \|\bar{\mathbf{w}}_{n-1} - \tilde{\mathbf{w}}_{k,n-1}\|^2} \leq \sqrt{\mathbb{E} \|\tilde{\mathbf{w}}_{n-1} - \bar{\mathbf{w}}_{n-1}\|^2} \\ & \leq \sqrt{\mathbb{E} \|\mathcal{V}_L \tilde{\mathbf{w}}_{n-1}\|^2} \leq \|\mathcal{V}_L\| \mu \check{c}_\epsilon = h \mu \end{aligned} \quad (119)$$

With regard to (d), we use the following inequality:

$$\sqrt{x} \leq \frac{1}{2}(x+1) \quad (120)$$

Combining (117) and (118), we have

$$\begin{aligned} & \mathbb{E} \left\{ \sum_k \pi_k \nabla_{\mathbf{w}^\top} J_k(\mathbf{w}_{k,n-1}) \bar{\mathbf{w}}_{n-1} \right\} \\ & \leq -(\nu - h \mu L^2) \sum_k \pi_k \mathbb{E} \|\tilde{\mathbf{w}}_{k,n-1}\|^2 + h \mu \left(O(\epsilon^2) + \frac{1}{2} \right) \end{aligned} \quad (121)$$

where $\nu - h \mu L^2 > 0$ when μ is sufficiently small. Now substituting (112), (115) and (121) into (111), and taking expectations on both sides of it gives

$$\begin{aligned} & \mathbb{E} \|\bar{\mathbf{w}}_n\|^2 \\ & \leq \mathbb{E} \|\bar{\mathbf{w}}_{n-1}\|^2 + 2h\mu^2 \left(O(\epsilon^2) + \frac{1}{2} \right) + O(\mu^2 \epsilon^2) + \mu^2 \sigma^2 - \end{aligned}$$

$$\begin{aligned} & (2\mu\nu - 2\mu^2 h L^2 - 2\mu^2 L^2 - \mu^2 \beta_{\max}^2) \sum_k \pi_k \mathbb{E} \|\tilde{\mathbf{w}}_{k,n-1}\|^2 \\ & \stackrel{(a)}{\leq} \mathbb{E} \|\bar{\mathbf{w}}_{n-1}\|^2 + 2h\mu^2 \left(O(\epsilon^2) + \frac{1}{2} \right) + O(\mu^2 \epsilon^2) + \mu^2 \sigma^2 - \\ & (2\mu\nu - 2\mu^2 h L^2 - 2\mu^2 L^2 - \mu^2 \beta_{\max}^2) \mathbb{E} \|\sum_k \pi_k \tilde{\mathbf{w}}_{k,n-1}\|^2 \\ & = \mathbb{E} \|\bar{\mathbf{w}}_{n-1}\|^2 + 2h\mu^2 \left(O(\epsilon^2) + \frac{1}{2} \right) + O(\mu^2 \epsilon^2) + \mu^2 \sigma^2 - \\ & (2\mu\nu - 2\mu^2 h L^2 - 2\mu^2 L^2 - \mu^2 \beta_{\max}^2) \mathbb{E} \|\bar{\mathbf{w}}_{n-1}\|^2 \\ & = \lambda \mathbb{E} \|\bar{\mathbf{w}}_{n-1}\|^2 + \mu^2 \check{c}_\epsilon^2 \end{aligned} \quad (122)$$

where (a) follows from Jensen's inequality, and

$$0 < \lambda = 1 - 2\mu\nu + 2\mu^2 h L^2 + 2\mu^2 L^2 + \mu^2 \beta_{\max}^2 < 1 \quad (123)$$

when μ is sufficiently small. Also,

$$\check{c}_\epsilon^2 = 2h \left(O(\epsilon^2) + \frac{1}{2} \right) + O(\epsilon^2) + \sigma^2 \quad (124)$$

Iterating (122), and after enough iterations \bar{n} with

$$\bar{n} \geq O \left(\frac{\log \mu}{\log(1 - O(\mu))} \right) \quad (125)$$

we have

$$\limsup_{n \rightarrow \infty} \mathbb{E} \|\bar{\mathbf{w}}_n\|^2 \leq 2\mu \frac{\check{c}_\epsilon^2}{1 - \lambda} = O(\mu) \quad (126)$$

Combining (108), (110), (125), and (126), we conclude that after enough iterations n with

$$\begin{aligned} n = \bar{n} + \bar{n} & \geq O \left(\frac{\log \mu}{\log(t + O(\mu^2))} \right) + O \left(\frac{\log \mu}{\log(1 - O(\mu))} \right) \\ & \stackrel{(a)}{=} O \left(\frac{\log \mu}{\log(1 - O(\mu))} \right) \end{aligned} \quad (127)$$

where (a) follows from the following equality:

$$\lim_{\mu \rightarrow 0} \frac{\log \mu}{\log(t + O(\mu^2))} = 0 \quad (128)$$

we have

$$\begin{aligned} \limsup_{n \rightarrow \infty} \mathbb{E} \|\tilde{\mathbf{w}}_n\|^2 &= \limsup_{n \rightarrow \infty} \mathbb{E} \|\mathcal{V}_\alpha^{-\top} \mathcal{V}_\alpha^\top \tilde{\mathbf{w}}_n\|^2 \\ & \stackrel{(a)}{\leq} \limsup_{n \rightarrow \infty} \|\mathcal{V}_\alpha^{-\top}\|^2 \left\{ \mathbb{E} \|\bar{\mathbf{w}}_n\|^2 + \mathbb{E} \|\tilde{\mathbf{w}}_n\|^2 \right\} \\ & \leq \check{c}_\epsilon^2 \mu = O(\mu) \end{aligned} \quad (129)$$

where (a) follows from (32), and

$$\check{c}_\epsilon^2 = \|\mathcal{V}_\alpha^{-\top}\|^2 \left(\frac{2\check{c}_\epsilon^2}{1 - \lambda} + \mu \check{c}_\epsilon^2 \right) \quad (130)$$

Note from (127) that the convergence speed of $\mathbb{E} \|\bar{\mathbf{w}}\|^2$ dominates the convergence of $\mathbb{E} \|\tilde{\mathbf{w}}_n\|^2$, thus $\mathbb{E} \|\tilde{\mathbf{w}}_n\|^2$ converges linearly with rate λ . \square

APPENDIX D
PROOF OF LEMMA 3

Proof. We first list two properties for the gradient noise over a batch of data for later use. By using the same method used to prove (86) and (92), we can verify that the stochastic gradient is unbiased with bounded second-order moment, i.e., it holds that:

$$\mathbb{E} \left\{ \bar{\mathbf{s}}_{k,n}^B \mid \mathcal{F}_{n-1} \right\} = 0 \quad (131)$$

$$\mathbb{E} \left\{ \left\| \bar{\mathbf{s}}_{k,n}^B(\mathbf{w}_{k,n-1}) \right\|^2 \mid \mathcal{F}_{n-1} \right\} \leq \frac{1}{B} (\beta^2 G^2 + \sigma^2) \quad (132)$$

Next, we analyze the difference between the iterates at the agents and the centroid. To begin with, the block centroid $\mathbf{w}_{c,n}$ satisfies the following relation:

$$\begin{aligned} \mathbf{w}_{c,n} &= \mathbb{1} \otimes \mathbf{w}_{c,n} = (\mathbb{1}\pi^\top \otimes I) \mathbf{w}_n \\ &\stackrel{(a)}{=} (\mathbb{1}\pi^\top \otimes I) (\mathbf{w}_{n-1} - \mu \mathcal{G}_{n-1} - \mu \bar{\mathbf{s}}_n^B) \end{aligned} \quad (133)$$

where (a) follows from (55) and (7). We thus obtain the following recursion which relates for the network disagreement:

$$\begin{aligned} \mathbf{w}_n - \mathbf{w}_{c,n} &= (\mathcal{A}^\top - \mathbb{1}\pi^\top \otimes I) (\mathbf{w}_{n-1} - \mu \mathcal{G}_{n-1} - \mu \bar{\mathbf{s}}_n^B) \\ &\stackrel{(a)}{=} (\mathcal{A}^\top - \mathbb{1}\pi^\top \otimes I) (I - \mathbb{1}\pi^\top \otimes I) (\mathbf{w}_{n-1} - \mu \mathcal{G}_{n-1} - \mu \bar{\mathbf{s}}_n^B) \\ &= (\mathcal{A}^\top - \mathbb{1}\pi^\top \otimes I) (I - \mathbb{1}\pi^\top \otimes I) \mathbf{w}_{n-1} - \\ &\quad (\mathcal{A}^\top - \mathbb{1}\pi^\top \otimes I) (I - \mathbb{1}\pi^\top \otimes I) \mu (\mathcal{G}_{n-1} + \bar{\mathbf{s}}_n^B) \\ &= (\mathcal{A}^\top - \mathbb{1}\pi^\top \otimes I) (\mathbf{w}_{n-1} - \mathbf{w}_{c,n-1} - \mu \mathcal{G}_{n-1} - \mu \bar{\mathbf{s}}_n^B) \end{aligned} \quad (134)$$

where (a) follows from

$$\mathcal{A}^\top - \mathbb{1}\pi^\top \otimes I = (\mathcal{A}^\top - \mathbb{1}\pi^\top \otimes I) (I - \mathbb{1}\pi^\top \otimes I) \quad (135)$$

Using eigen-structure of the combination matrix A from (26)–(31c), we have

$$\mathcal{A}^\top - \mathbb{1}\pi^\top \otimes I_M = (\mathcal{V}_\alpha^\top)^{-1} \tilde{\mathcal{J}}^\top \mathcal{V}_\alpha^\top \quad (136)$$

where

$$\tilde{\mathcal{J}} = \tilde{\mathcal{J}} \otimes I_M = \begin{bmatrix} 0 & 0 \\ 0 & J_\alpha \end{bmatrix} \otimes I_M \quad (137)$$

Now consider

$$\bar{\mathbf{w}}_n \triangleq \mathcal{V}_\alpha^\top (\mathbf{w}_n - \mathbf{w}_{c,n}) \quad (138)$$

and substituting (134) into it, we get

$$\begin{aligned} \|\bar{\mathbf{w}}_n\|^2 &= \|\mathcal{V}_\alpha^\top (\mathbf{w}_n - \mathbf{w}_{c,n})\|^2 \\ &= \left\| \mathcal{V}_\alpha^\top \left((\mathcal{V}_\alpha^\top)^{-1} \tilde{\mathcal{J}}^\top \mathcal{V}_\alpha^\top (\mathbf{w}_{n-1} - \mathbf{w}_{c,n-1} - \mu \mathcal{G}_{n-1} - \mu \bar{\mathbf{s}}_n^B) \right) \right\|^2 \\ &= \left\| \tilde{\mathcal{J}}^\top \bar{\mathbf{w}}_{n-1} - \mu \tilde{\mathcal{J}}^\top \mathcal{V}_\alpha^\top (\mathcal{G}_{n-1} + \bar{\mathbf{s}}_n^B) \right\|^2 \\ &= \left\| t \frac{1}{t} \tilde{\mathcal{J}}^\top \bar{\mathbf{w}}_{n-1} - (1-t) \frac{\mu}{1-t} \tilde{\mathcal{J}}^\top \mathcal{V}_\alpha^\top (\mathcal{G}_{n-1} + \bar{\mathbf{s}}_n^B) \right\|^2 \\ &\stackrel{(a)}{\leq} \frac{1}{t} \left\| \tilde{\mathcal{J}}^\top \right\|^2 \|\bar{\mathbf{w}}_{n-1}\|^2 + \frac{\mu^2 \left\| \tilde{\mathcal{J}}^\top \right\|^2 \|\mathcal{V}_\alpha^\top\|^2}{1-t} \|\mathcal{G}_{n-1} + \bar{\mathbf{s}}_n^B\|^2 \end{aligned} \quad (139)$$

where (a) follows from Jensen's inequality for any $0 < t < 1$. Similar to (94), we select

$$t = \left\| \tilde{\mathcal{J}}^\top \right\| = \|J_\alpha^\top\| = \sqrt{\tau(J_\alpha J_\alpha^\top)} = \lambda_2 + \alpha < 1 \quad (140)$$

where α is arbitrarily small to guarantee the rightmost inequality. Then, we have

$$\begin{aligned} &\mathbb{E} \left\{ \|\bar{\mathbf{w}}_n\|^2 \mid \mathcal{F}_{n-1} \right\} \\ &\stackrel{(a)}{\leq} t \|\bar{\mathbf{w}}_{n-1}\|^2 + \frac{\mu^2 t^2 \|\mathcal{V}_\alpha^\top\|^2}{1-t} \mathbb{E} \left\{ \sum_{k=1}^K \|\nabla_w J_k(\mathbf{w}_{k,n-1}) + \bar{\mathbf{s}}_{k,n}^B\|^2 \mid \mathcal{F}_{n-1} \right\} \\ &\stackrel{(b)}{\leq} t \|\bar{\mathbf{w}}_{n-1}\|^2 + \frac{\mu^2 t^2 \|\mathcal{V}_\alpha^\top\|^2}{1-t} \mathbb{E} \left\{ \sum_{k=1}^K \|\nabla_w J_k(\mathbf{w}_{k,n-1})\|^2 + \|\bar{\mathbf{s}}_{k,n}^B\|^2 \mid \mathcal{F}_{n-1} \right\} \\ &\stackrel{(c)}{\leq} t \|\bar{\mathbf{w}}_{n-1}\|^2 + \frac{\mu^2 t^2 \|\mathcal{V}_\alpha^\top\|^2}{1-t} K \left(G^2 + \frac{\beta^2 G^2 + \sigma^2}{B} \right) \end{aligned} \quad (141)$$

where (a) follows from (48) and (53), (b) follows from (131), and (c) follows from (132) and (44). Taking expectations of both sides, we arrive at

$$\begin{aligned} &\mathbb{E} \|\bar{\mathbf{w}}_n\|^2 \\ &\leq t \mathbb{E} \|\bar{\mathbf{w}}_{n-1}\|^2 + \frac{\mu^2 t^2 \|\mathcal{V}_\alpha^\top\|^2}{1-t} K \left(G^2 + \frac{\beta^2 G^2 + \sigma^2}{B} \right) \end{aligned} \quad (142)$$

Then after enough iterations n_0 such that

$$\begin{aligned} t^{n_0+1} \mathbb{E} \|\bar{\mathbf{w}}_{-1}\|^2 &\leq \frac{\mu^2 t^2 \|\mathcal{V}_\alpha^\top\|^2 \|(\mathcal{V}_\alpha^\top)^{-1}\|^2}{(1-t)^2} K \\ &\quad \times \left(G^2 + \frac{\beta^2 G^2 + \sigma^2}{B} \right) \end{aligned}$$

which is equivalent to

$$n_0 \geq O \left(\frac{\log \mu}{\log t} \right) \quad (143)$$

we get

$$\begin{aligned} \mathbb{E} \|\mathbf{w}_n - \mathbf{w}_{c,n}\|^2 &= \mathbb{E} \|(\mathcal{V}_\alpha^\top)^{-1} \bar{\mathbf{w}}_n\|^2 \\ &\leq \frac{2\mu^2 t^2 \|\mathcal{V}_\alpha^\top\|^2 \|(\mathcal{V}_\alpha^\top)^{-1}\|^2}{(1-t)^2} K \left(G^2 + \frac{\beta^2 G^2 + \sigma^2}{B} \right) \end{aligned} \quad (144)$$

$$\stackrel{(a)}{\leq} \frac{2\mu^2 t^2 \|\mathcal{V}_\alpha^\top\|^2 \|(\mathcal{V}_\alpha^\top)^{-1}\|^2}{(1-t)^2} K \left(G^2 + \frac{\beta^2 G^2 + \sigma^2}{B} \right) \quad (145)$$

Furthermore,

$$\begin{aligned} &\mathbb{E} \|\mathbf{w}_{k,n} - \mathbf{w}_{c,n}\| \\ &\leq (\mathbb{E} \|\mathbf{w}_{k,n} - \mathbf{w}_{c,n}\|^2)^{\frac{1}{2}} \\ &\leq (\mathbb{E} \|\mathbf{w}_n - \mathbf{w}_{c,n}\|^2)^{\frac{1}{2}} \end{aligned}$$

$$\leq \frac{\mu t \|\mathcal{V}_\alpha^T\| \|(\mathcal{V}_\alpha^T)^{-1}\|}{(1-t)} \sqrt{K \left(G^2 + \frac{\beta^2 G^2 + \sigma^2}{|B|} \right)} \quad (146)$$

□

APPENDIX E
PROOF OF LEMMA 4

Proof. From (85) and (63), we know that

$$\begin{aligned} \mathbb{E} \left\{ \widehat{\mathbf{s}}_n^B | \mathcal{F}_{n-1} \right\} &= \mathbb{E} \left\{ \sum_k \pi_k \bar{\mathbf{s}}_{k,n}^B | \mathcal{F}_{n-1} \right\} \\ &= \sum_k \pi_k \mathbb{E} \left\{ \bar{\mathbf{s}}_{k,n}^B | \mathcal{F}_{n-1} \right\} \\ &= 0 \end{aligned} \quad (147)$$

Moreover, expression (132) gives

$$\begin{aligned} \mathbb{E} \left\{ \left\| \widehat{\mathbf{s}}_n^B \right\|^2 \right\} &= \mathbb{E} \left\{ \mathbb{E} \left\{ \left\| \widehat{\mathbf{s}}_n^B \right\|^2 | \mathcal{F}_{n-1} \right\} \right\} \\ &= \mathbb{E} \left\{ \mathbb{E} \left\{ \left\| \sum_k \pi_k \bar{\mathbf{s}}_{k,n}^B \right\|^2 | \mathcal{F}_{n-1} \right\} \right\} \\ &\stackrel{(a)}{\leq} \mathbb{E} \left\{ \mathbb{E} \left\{ \sum_k \pi_k \left\| \bar{\mathbf{s}}_{k,n}^B \right\|^2 | \mathcal{F}_{n-1} \right\} \right\} \\ &\leq \frac{1}{B} (\beta^2 G^2 + \sigma^2) \end{aligned} \quad (148)$$

where (a) follows from Jensen's inequality.

As for \mathbf{d}_{n-1} , after enough iterations n_0 , we get

$$\begin{aligned} \mathbb{E} \left\| \mathbf{d}_{n-1} \right\|^2 &= \mathbb{E} \left\| \sum_{k=1}^K \pi_k \mathbf{d}_{k,n-1} \right\|^2 \\ &\stackrel{(a)}{\leq} \sum_k \pi_k \mathbb{E} \left\| \overline{\nabla_w J_k}(\mathbf{w}_{k,n-1}) - \overline{\nabla_w J_k}(\mathbf{w}_{c,n-1}) \right\|^2 \\ &\stackrel{(b)}{\leq} \sum_k \pi_k L^2 \mathbb{E} \left\| \mathbf{w}_{k,n-1} - \mathbf{w}_{c,n-1} \right\|^2 \\ &\leq \pi_{\max} L^2 \mathbb{E} \left\| \mathbf{w}_{n-1} - \mathbf{w}_{c,n-1} \right\|^2 \\ &\stackrel{(c)}{\leq} \pi_{\max} L^2 \frac{2\mu^2 t^2 \|\mathcal{V}_\alpha^T\|^2 \|(\mathcal{V}_\alpha^T)^{-1}\|^2}{(1-t)^2} K \left(G^2 + \frac{\beta^2 G^2 + \sigma^2}{B} \right) \end{aligned} \quad (149)$$

where (a) follows from Jensen's inequality, (b) follows from (8a), (c) follows from (144), and π_{\max} is the largest entry of π . □

APPENDIX F
PROOF OF THEOREM 2

Proof. One difficulty in the analysis of the convergence of the adversarial diffusion strategy (43a)–(43c) is due to the non-smoothness of $J(w)$. Thus, we resort to the Moreau envelope method and L -weak convexity [30], [33], [34], [39], [40] to study near-stationarity for non-smooth loss functions. Consider function $f(z; w)$ defined by

$$f(z; w) \triangleq J(z) + \frac{1}{2\gamma} \|w - z\|^2 \quad (150)$$

We already know from [30] that the maximum function $g(z)$ in (4) is L -weakly convex if (8a) is satisfied. Therefore, its expectation $J(z)$ is also L -weakly convex so that $f(z; w)$ is strongly convex over z if $\gamma < \frac{1}{L}$. Then, the Moreau envelope of $J(w)$ is defined by [4]:

$$J_\gamma(w) \triangleq \min_z f(z; w) \quad (151)$$

Let

$$\widehat{z} = \operatorname{argmin}_z f(z; w) \quad (152)$$

then \widehat{z} is uniquely determined by w since $f(z; w)$ is strongly convex. Even when $J(z)$ is non-differentiable, the Moreau envelope will be differentiable relative to w . In particular, it holds that [4], [33]:

$$\frac{1}{\gamma} (w - \widehat{z}) = \nabla_w J_\gamma(w) \quad (153a)$$

$$\nabla_w J_\gamma(w) \in \partial_w J(\widehat{z}) \quad (153b)$$

It follows that if $J_\gamma(w)$ arrives at an approximate stationary point w^o , i.e., if $\|\nabla_w J_\gamma(w^o)\|^2$ is bounded by a small value κ^2 , then

$$\min_{\zeta \in \partial_w J(\widehat{z}^o)} \|\zeta\|^2 \leq \|w^o - \widehat{z}^o\|^2 = \gamma^2 \|\nabla_w J_\gamma(w^o)\|^2 \leq \gamma^2 \kappa^2 \quad (154)$$

where

$$\widehat{z}^o = \operatorname{argmin}_z f(z; w^o) \quad (155)$$

which implies that w^o is $O(\kappa^2)$ near a κ^2 -approximate stationary point of $J(w)$. Thus, it is reasonable to treat $\nabla_w J_\gamma(w)$ as a surrogate for $\partial_w J(w)$. Consider the proximal operator associated with the original risk from (2) at location $\mathbf{w}_{c,n-1}$:

$$\widehat{\mathbf{w}}_{n-1} = \operatorname{argmin}_z \left\{ J(z) + \left(L + \frac{1}{2} \right) \|z - \mathbf{w}_{c,n-1}\|^2 \right\} \quad (156)$$

The resulting Moreau envelope is given by:

$$J_{\frac{1}{2L+1}}(\mathbf{w}_{c,n-1}) = \min_z J(z) + \left(L + \frac{1}{2} \right) \|z - \mathbf{w}_{c,n-1}\|^2 \quad (157)$$

We know from expression (175) in Appendix G that

$$\begin{aligned} &\overline{\nabla_{w^\top} J_k}(\mathbf{w}_{c,n-1})(\widehat{\mathbf{w}}_{n-1} - \mathbf{w}_{c,n-1}) \\ &\leq J_k(\widehat{\mathbf{w}}_{n-1}) - J_k(\mathbf{w}_{c,n-1}) + \boldsymbol{\eta}_k + \frac{L}{2} \|\widehat{\mathbf{w}}_{n-1} - \mathbf{w}_{c,n-1}\|^2 \end{aligned} \quad (158)$$

where

$$\boldsymbol{\eta}_k \leq O(\epsilon_k) \|\mathbf{w} - \mathbf{w}_{c,n-1}\| + O(\epsilon_k^2) \quad (159)$$

It is argued in [30] that the function $g(w)$ defined by (4) can be L -weakly convex if (8a) is satisfied. It follows that the the function $g(w) + (L + \frac{1}{2}) \|w\|^2$ is $(L + 1)$ -strongly-convex over w and its expectation $J(w) + (L + \frac{1}{2}) \|w\|^2$ is

also $(L + 1)$ -strongly-convex. This implies that

$$\begin{aligned}
& J(\mathbf{w}_{c,n-1}) - J(\widehat{\mathbf{w}}_{n-1}) - \frac{1}{2}(L + 1) \|\mathbf{w}_{c,n-1} - \widehat{\mathbf{w}}_{n-1}\|^2 \\
&= J(\mathbf{w}_{c,n-1}) + \left(L + \frac{1}{2}\right) \|\mathbf{w}_{c,n-1} - \mathbf{w}_{c,n-1}\|^2 - J(\widehat{\mathbf{w}}_{n-1}) \\
&\quad - \left(L + \frac{1}{2}\right) \|\mathbf{w}_{c,n-1} - \widehat{\mathbf{w}}_{n-1}\|^2 + \frac{L}{2} \|\mathbf{w}_{c,n-1} - \widehat{\mathbf{w}}_{n-1}\|^2 \\
&= J(\mathbf{w}_{c,n-1}) + \left(L + \frac{1}{2}\right) \|\mathbf{w}_{c,n-1} - \mathbf{w}_{c,n-1}\|^2 - \\
&\quad \min_{\mathbf{w}} \left\{ J(\mathbf{w}) + \left(L + \frac{1}{2}\right) \|\mathbf{w} - \mathbf{w}_{c,n-1}\|^2 \right\} \\
&\quad + \frac{L}{2} \|\mathbf{w}_{c,n-1} - \widehat{\mathbf{w}}_{n-1}\|^2 \\
&\stackrel{(a)}{\geq} \left(L + \frac{1}{2}\right) \|\mathbf{w}_{c,n-1} - \widehat{\mathbf{w}}_{n-1}\|^2 \\
&\stackrel{(b)}{=} \frac{1}{4L + 2} \left\| \nabla_w J_{\frac{1}{2L+1}}(\mathbf{w}_{c,n-1}) \right\|^2 \tag{160}
\end{aligned}$$

where (a) follows from the strong convexity of the function $J(\mathbf{w}) + (L + \frac{1}{2}) \|\mathbf{w}\|^2$, and (b) follows from (153a) with $\gamma = \frac{1}{2L+1}$. Then we get

$$\begin{aligned}
& J_{\frac{1}{2L+1}}(\mathbf{w}_{c,n}) = \min_{\mathbf{z}} J(\mathbf{z}) + \left(L + \frac{1}{2}\right) \|\mathbf{w}_{c,n} - \mathbf{z}\|^2 \\
&\leq J(\widehat{\mathbf{w}}_{n-1}) + \left(L + \frac{1}{2}\right) \|\mathbf{w}_{c,n} - \widehat{\mathbf{w}}_{n-1}\|^2 \\
&\stackrel{(a)}{=} J(\widehat{\mathbf{w}}_{n-1}) + \left(L + \frac{1}{2}\right) \left\| \mathbf{w}_{c,n-1} - \widehat{\mathbf{w}}_{n-1} - \mu \mathbf{d}_{n-1} - \mu \widehat{\mathbf{s}}_n^B \right. \\
&\quad \left. - \mu \sum_k \pi_k \overline{\nabla_w J_k}(\mathbf{w}_{c,n-1}) \right\|^2 \\
&= J(\widehat{\mathbf{w}}_{n-1}) + \left(L + \frac{1}{2}\right) \|\mathbf{w}_{c,n-1} - \widehat{\mathbf{w}}_{n-1}\|^2 + 2\mu \left(L + \frac{1}{2}\right) \times \\
&\quad \left(\mathbf{d}_{n-1} + \widehat{\mathbf{s}}_n^B + \sum_k \pi_k \overline{\nabla_w J_k}(\mathbf{w}_{c,n-1}) \right)^\top (\widehat{\mathbf{w}}_{n-1} - \mathbf{w}_{c,n-1}) \\
&\quad + \mu^2 \left(L + \frac{1}{2}\right) \left\| \sum_k \pi_k \overline{\nabla_w J_k}(\mathbf{w}_{c,n-1}) + \mathbf{d}_{n-1} + \widehat{\mathbf{s}}_n^B \right\|^2 \\
&\stackrel{(b)}{\leq} J_{\frac{1}{2L+1}}(\mathbf{w}_{c,n-1}) \\
&\quad + 2\mu \left(L + \frac{1}{2}\right) (\mathbf{d}_{n-1} + \widehat{\mathbf{s}}_n^B)^\top (\widehat{\mathbf{w}}_{n-1} - \mathbf{w}_{c,n-1}) \\
&\quad + 2\mu \left(L + \frac{1}{2}\right) \left(\sum_k \pi_k J_k(\widehat{\mathbf{w}}_{n-1}) - \sum_k \pi_k J_k(\mathbf{w}_{c,n-1}) \right. \\
&\quad \left. + \sum_k \pi_k \boldsymbol{\eta}_k + \frac{L}{2} \|\widehat{\mathbf{w}}_{n-1} - \mathbf{w}_{c,n-1}\|^2 \right) \\
&\quad + \mu^2 \left(L + \frac{1}{2}\right) \left\| \sum_k \pi_k \overline{\nabla_w J_k}(\mathbf{w}_{c,n-1}) + \mathbf{d}_{n-1} + \widehat{\mathbf{s}}_n^B \right\|^2 \\
&\leq J_{\frac{1}{2L+1}}(\mathbf{w}_{c,n-1}) + 2\mu \left(L + \frac{1}{2}\right) \left(J(\widehat{\mathbf{w}}_{n-1}) - J(\mathbf{w}_{c,n-1}) \right. \\
&\quad \left. + \boldsymbol{\eta} + \frac{L}{2} \|\widehat{\mathbf{w}}_{n-1} - \mathbf{w}_{c,n-1}\|^2 \right)
\end{aligned}$$

$$\begin{aligned}
& + 2\mu \left(L + \frac{1}{2}\right) (\mathbf{d}_{n-1} + \widehat{\mathbf{s}}_n^B)^\top (\widehat{\mathbf{w}}_{n-1} - \mathbf{w}_{c,n-1}) \\
& + \mu^2 \left(L + \frac{1}{2}\right) \left\| \sum_k \pi_k \overline{\nabla_w J_k}(\mathbf{w}_{c,n-1}) + \mathbf{d}_{n-1} + \widehat{\mathbf{s}}_n^B \right\|^2 \tag{161}
\end{aligned}$$

where (a) follows from (61), (b) follows from (158), and

$$\begin{aligned}
\boldsymbol{\eta} &= \sum_k \pi_k \boldsymbol{\eta}_k \\
&\leq O(\epsilon) \sum_k \pi_k \|\mathbf{w}_{k,n-1} - \mathbf{w}_{c,n-1}\| + O(\epsilon^2) \tag{162}
\end{aligned}$$

follows from (176). Then, conditioning both side of (161) and substituting (147) into it, we get

$$\begin{aligned}
& \mathbb{E} \left\{ J_{\frac{1}{2L+1}}(\mathbf{w}_{c,n}) | \mathcal{F}_{n-1} \right\} \\
&\leq J_{\frac{1}{2L+1}}(\mathbf{w}_{c,n-1}) + 2\mu \left(L + \frac{1}{2}\right) \left(J(\widehat{\mathbf{w}}_{n-1}) - J(\mathbf{w}_{c,n-1}) \right. \\
&\quad \left. + \boldsymbol{\eta} + \frac{1}{2}(L + 1) \|\widehat{\mathbf{w}}_{n-1} - \mathbf{w}_{c,n-1}\|^2 \right) \\
&\quad + \mu \left(L + \frac{1}{2}\right) \mathbb{E} \left\{ \|\mathbf{d}_{n-1}\|^2 | \mathcal{F}_{n-1} \right\} \\
&\quad + \mu^2 \left(L + \frac{1}{2}\right) \mathbb{E} \left\{ 2 \left\| \sum_k \pi_k \overline{\nabla_w J_k}(\mathbf{w}_{c,n-1}) \right\|^2 \right. \\
&\quad \left. + 2 \|\mathbf{d}_{n-1}\|^2 + \|\widehat{\mathbf{s}}_n^B\|^2 | \mathcal{F}_{n-1} \right\} \tag{163}
\end{aligned}$$

where we use the inequality

$$\mathbf{d}_{n-1}^\top (\widehat{\mathbf{w}}_{n-1} - \mathbf{w}_{c,n-1}) \leq \frac{1}{2} \|\mathbf{d}_{n-1}\|^2 + \frac{1}{2} \|\widehat{\mathbf{w}}_{n-1} - \mathbf{w}_{c,n-1}\|^2 \tag{164}$$

Taking the expectation of both sides of (163), we obtain

$$\begin{aligned}
& \mathbb{E} J_{\frac{1}{2L+1}}(\mathbf{w}_{c,n}) \\
&\leq \mathbb{E} J_{\frac{1}{2L+1}}(\mathbf{w}_{c,n-1}) + 2\mu \left(L + \frac{1}{2}\right) \mathbb{E} \left\{ J(\widehat{\mathbf{w}}_{n-1}) - J(\mathbf{w}_{c,n-1}) \right. \\
&\quad \left. + \boldsymbol{\eta} + \frac{1}{2}(L + 1) \|\widehat{\mathbf{w}}_{n-1} - \mathbf{w}_{c,n-1}\|^2 \right\} \\
&\quad + \mu^2 \left(L + \frac{1}{2}\right) \mathbb{E} \|\widehat{\mathbf{s}}_n^B\|^2 \\
&\quad + 2\mu^2 \left(L + \frac{1}{2}\right) \mathbb{E} \left\| \sum_k \pi_k \overline{\nabla_w J_k}(\mathbf{w}_{c,n-1}) \right\|^2 \\
&\quad + (\mu + 2\mu^2) \left(L + \frac{1}{2}\right) \mathbb{E} \|\mathbf{d}_{n-1}\|^2 \tag{165}
\end{aligned}$$

Then substituting (160) into (165), we have

$$\begin{aligned}
& 2\mu \left(L + \frac{1}{2}\right) \cdot \frac{1}{4L + 2} \mathbb{E} \left\| \nabla_w J_{\frac{1}{2L+1}}(\mathbf{w}_{c,n-1}) \right\|^2 \\
&\leq 2\mu \left(L + \frac{1}{2}\right) \cdot \mathbb{E} \left\{ J(\mathbf{w}_{c,n-1}) - J(\widehat{\mathbf{w}}_{n-1}) - \right. \\
&\quad \left. \frac{1}{2}(L + 1) \|\widehat{\mathbf{w}}_{n-1} - \mathbf{w}_{c,n-1}\|^2 \right\}
\end{aligned}$$

$$\begin{aligned}
&\leq \mathbb{E} J_{\frac{1}{2L+1}}(\mathbf{w}_{c,n-1}) - \mathbb{E} J_{\frac{1}{2L+1}}(\mathbf{w}_{c,n}) + 2\mu \left(L + \frac{1}{2} \right) \mathbb{E} \eta \\
&\quad + 2\mu^2 \left(L + \frac{1}{2} \right) \mathbb{E} \left\| \sum_k \pi_k \overline{\nabla_w J_k}(\mathbf{w}_{c,n-1}) \right\|^2 \\
&\quad + (\mu + 2\mu^2) \left(L + \frac{1}{2} \right) \mathbb{E} \|\mathbf{d}_{n-1}\|^2 + \mu^2 \left(L + \frac{1}{2} \right) \mathbb{E} \|\widehat{\mathbf{s}}_n^B\|^2
\end{aligned} \tag{166}$$

Substituting (44), (146), (148), and (149) into (166), after sufficient iterations \widehat{N} , we obtain

$$\begin{aligned}
&\frac{1}{\widehat{N}} \sum_n \mathbb{E} \|\nabla_w J_{\frac{1}{2L+1}}(\mathbf{w}_{c,n-1})\|^2 \\
&\leq \frac{2(J_{\frac{1}{2L+1}}(\mathbf{w}_{c,n_0}) - \Delta)}{\mu \widehat{N}} + O(\mu) + O(\epsilon^2)
\end{aligned} \tag{167}$$

where $\Delta = \min_w J(\mathbf{w})$. This implies that $\exists n_0 \leq N \leq \widehat{N}$, for which we have

$$\begin{aligned}
&\mathbb{E} \|\nabla_w J_{\frac{1}{2L+1}}(\mathbf{w}_{c,N-1})\|^2 \\
&\leq \frac{2(J_{\frac{1}{2L+1}}(\mathbf{w}_{c,n_0}) - \Delta)}{\mu \widehat{N}} + O(\mu) + O(\epsilon^2)
\end{aligned} \tag{168}$$

Then, according to (154), we have

$$\begin{aligned}
&\mathbb{E} \left\{ \min_{\zeta \in \partial_w J(\widehat{\mathbf{w}}_{N-1})} \|\zeta\|^2 \right\} \leq \mathbb{E} \|\nabla_w J_{\frac{1}{2L+1}}(\mathbf{w}_{c,N-1})\|^2 \\
&\leq \frac{2(J_{\frac{1}{2L+1}}(\mathbf{w}_{c,n_0}) - \Delta)}{\mu \widehat{N}} + O(\mu) + O(\epsilon^2)
\end{aligned} \tag{169}$$

and

$$\|\widehat{\mathbf{w}}_{N-1} - \mathbf{w}_{c,N-1}\|^2 \leq \frac{2(J_{\frac{1}{2L+1}}(\mathbf{w}_{c,n_0}) - \Delta)}{\mu \widehat{N}} + O(\mu) + O(\epsilon^2) \tag{170}$$

APPENDIX G PROOF OF (158)

Proof. Note that

$$\begin{aligned}
&Q_k(\mathbf{w}_c; \mathbf{x}_k + \delta_k^*, \mathbf{y}_k) - Q_k(\mathbf{w}_c; \mathbf{x}_k + \widehat{\delta}_k, \mathbf{y}_k) \\
&\stackrel{(a)}{\leq} \nabla_{\mathbf{x}^\top} Q_k(\mathbf{w}_c; \mathbf{x}_k + \widehat{\delta}_k, \mathbf{y}_k) (\delta_k^* - \widehat{\delta}_k) + \frac{L}{2} \|\delta_k^* - \widehat{\delta}_k\|^2 \\
&= \left(\nabla_x Q_k(\mathbf{w}_c; \mathbf{x}_k + \widehat{\delta}_k, \mathbf{y}_k) - \nabla_x Q_k(\mathbf{w}_k; \mathbf{x}_k + \widehat{\delta}_k, \mathbf{y}_k) \right)^\top \\
&\quad \times (\delta_k^* - \widehat{\delta}_k) + \left(\nabla_x Q_k(\mathbf{w}_k; \mathbf{x}_k + \widehat{\delta}_k, \mathbf{y}_k) \right. \\
&\quad \left. - \nabla_x Q_k(\mathbf{w}_k; \mathbf{x}_k, \mathbf{y}_k) \right)^\top (\delta_k^* - \widehat{\delta}_k) \\
&\quad + \nabla_{\mathbf{x}^\top} Q_k(\mathbf{w}_k; \mathbf{x}_k, \mathbf{y}_k) (\delta_k^* - \widehat{\delta}_k) + \frac{L}{2} \|\delta_k^* - \widehat{\delta}_k\|^2 \\
&\stackrel{(b)}{\leq} \|\nabla_x Q_k(\mathbf{w}_c; \mathbf{x}_k + \widehat{\delta}_k, \mathbf{y}_k) - \nabla_x Q_k(\mathbf{w}_k; \mathbf{x}_k + \widehat{\delta}_k, \mathbf{y}_k)\| \\
&\quad \times \|\delta_k^* - \widehat{\delta}_k\| + \|\nabla_x Q_k(\mathbf{w}_k; \mathbf{x}_k + \widehat{\delta}_k, \mathbf{y}_k) \\
&\quad - \nabla_x Q_k(\mathbf{w}_k; \mathbf{x}_k, \mathbf{y}_k)\| \|\delta_k^* - \widehat{\delta}_k\| + \frac{L}{2} \|\delta_k^* - \widehat{\delta}_k\|^2
\end{aligned}$$

$$\begin{aligned}
&\stackrel{(c)}{\leq} (L \|\mathbf{w}_k - \mathbf{w}_c\| + L \|\widehat{\delta}_k\|) \|\delta_k^* - \widehat{\delta}_k\| + \frac{L}{2} \|\delta_k^* - \widehat{\delta}_k\|^2 \\
&\leq \|\mathbf{w}_k - \mathbf{w}_c\| O(\epsilon_k) + O(\epsilon_k^2)
\end{aligned} \tag{171}$$

where (a) and (c) follow from the Lipschitz conditions in Assumption 2, (b) is due to

$$\widehat{\delta}_k = \operatorname{argmax}_{\|\delta_k\|_{p_k} \leq \epsilon_k} \delta_k^\top \nabla_x Q_k(\mathbf{w}_k; \mathbf{x}_k, \mathbf{y}_k) \tag{172}$$

where $\widehat{\delta}_k$ is the exact maximizer of the linear approximation, so that we have

$$\nabla_{\mathbf{x}^\top} Q_k(\mathbf{w}_k; \mathbf{x}_k, \mathbf{y}_k) (\delta_k^* - \widehat{\delta}_k) \leq 0 \tag{173}$$

Meanwhile,

$$\delta_k^* = \operatorname{argmax}_{\|\delta_k\|_{p_k} \leq \epsilon_k} Q_k(\mathbf{w}_c; \mathbf{x}_k + \delta_k, \mathbf{y}_k) \tag{174}$$

is the true maximizer for \mathbf{w}_c . Then for any $\mathbf{w} \in \mathcal{F}_{n-1}$, we have

$$\begin{aligned}
J_k(\mathbf{w}) &= \mathbb{E}_{\{\mathbf{x}_k, \mathbf{y}_k\}} \left\{ \max_{\|\delta_k\|_{p_k} \leq \epsilon_k} Q_k(\mathbf{w}; \mathbf{x}_k + \delta_k, \mathbf{y}_k) \right\} \\
&\geq \mathbb{E}_{\{\mathbf{x}_k, \mathbf{y}_k\}} Q_k(\mathbf{w}; \widehat{\mathbf{x}}_k, \mathbf{y}_k) \\
&\stackrel{(a)}{\geq} \mathbb{E}_{\{\mathbf{x}_k, \mathbf{y}_k\}} Q_k(\mathbf{w}_{c,n-1}; \widehat{\mathbf{x}}_k, \mathbf{y}_k) - \frac{L}{2} \|\mathbf{w} - \mathbf{w}_{c,n-1}\|^2 \\
&\quad + \mathbb{E}_{\{\mathbf{x}_k, \mathbf{y}_k\}} \nabla_{\mathbf{w}^\top} Q_k(\mathbf{w}_{c,n-1}; \widehat{\mathbf{x}}_k, \mathbf{y}_k) (\mathbf{w} - \mathbf{w}_{c,n-1}) \\
&= \mathbb{E}_{\{\mathbf{x}_k, \mathbf{y}_k\}} Q_k(\mathbf{w}_{c,n-1}; \widehat{\mathbf{x}}_k, \mathbf{y}_k) - \frac{L}{2} \|\mathbf{w} - \mathbf{w}_{c,n-1}\|^2 \\
&\quad + \overline{\nabla_{\mathbf{w}^\top} J_k}(\mathbf{w}_{c,n-1}) (\mathbf{w} - \mathbf{w}_{c,n-1}) \\
&\stackrel{(b)}{\geq} \mathbb{E}_{\{\mathbf{x}_k, \mathbf{y}_k\}} \left\{ \max_{\|\delta_k\|_{p_k} \leq \epsilon_k} Q_k(\mathbf{w}_{c,n-1}; \mathbf{x}_k + \delta_k, \mathbf{y}_k) \right\} - \eta_k \\
&\quad - \frac{L}{2} \|\mathbf{w} - \mathbf{w}_{c,n-1}\|^2 + \overline{\nabla_{\mathbf{w}^\top} J_k}(\mathbf{w}_{c,n-1}) (\mathbf{w} - \mathbf{w}_{c,n-1}) \\
&= J_k(\mathbf{w}_{c,n-1}) - \eta_k - \frac{L}{2} \|\mathbf{w} - \mathbf{w}_{c,n-1}\|^2 \\
&\quad + \overline{\nabla_{\mathbf{w}^\top} J_k}(\mathbf{w}_{c,n-1}) (\mathbf{w} - \mathbf{w}_{c,n-1})
\end{aligned} \tag{175}$$

where (a) follows from the L-weak convexity of $Q(\cdot)$ over \mathbf{w} , (b) follows from (171), and

$$\eta_k \leq O(\epsilon_k) \|\mathbf{w} - \mathbf{w}_{c,n-1}\| + O(\epsilon_k^2) \tag{176}$$

$$\widehat{\mathbf{x}}_k = \mathbf{x}_k + \operatorname{argmax}_{\|\delta_k\|_{p_k} \leq \epsilon_k} \delta_k^\top \nabla_x Q_k(\mathbf{w}_{c,n-1}; \mathbf{x}_k, \mathbf{y}_k) \tag{177}$$

where the perturbation added to \mathbf{x}_k is evaluated at $\mathbf{w}_{c,n-1}$. \square

REFERENCES

- [1] Y. Cao, E. Rizk, S. Vlaski, and A. H. Sayed, "Multi-agent adversarial training using diffusion learning," in *Proc. IEEE ICASSP*, pp. 1–5, Rhodes Island, June 2023.
- [2] C. Szegedy, W. Zaremba, I. Sutskever, J. Bruna, D. Erhan, I. Goodfellow, and R. Fergus, "Intriguing properties of neural networks," in *Proc. ICLR*, pp. 1–10, Banff, 2014.
- [3] T. Bai, J. Luo, J. Zhao, B. Wen, and Q. Wang, "Recent advances in adversarial training for adversarial robustness," in *Proc. IJCAI*, pp. 4312–4321, Montreal, 2021.
- [4] A. H. Sayed, *Inference and Learning from Data*. Cambridge University Press, 2022.

- [5] Y. Song, T. Kim, S. Nowozin, S. Ermon, and N. Kushman, "Pixeldefend: Leveraging generative models to understand and defend against adversarial examples," in *Proc. ICLR*, pp. 1–20, Vancouver, 2018.
- [6] D. Hendrycks, A. Zou, M. Mazeika, L. Tang, B. Li, D. Song, and J. Steinhardt, "Pixmix: Dreamlike pictures comprehensively improve safety measures," in *Proc. IEEE CVPR*, pp. 16762–16771, New Orleans, 2022.
- [7] T. Miyato, A. M. Dai, and I. Goodfellow, "Adversarial training methods for semi-supervised text classification," in *Proc. ICLR*, pp. 1–11, Toulon, 2017.
- [8] R. Jia and P. Liang, "Adversarial examples for evaluating reading comprehension systems," in *Proc. EMNLP*, pp. 1–11, Copenhagen, 2017.
- [9] L. Pinto, J. Davidson, R. Sukthankar, and A. Gupta, "Robust adversarial reinforcement learning," in *Proc. ICML*, pp. 2817–2826, Sydney, 2017.
- [10] S. Gu and L. Rigazio, "Towards deep neural network architectures robust to adversarial examples," in *Proc. ICLR Workshop*, pp. 1–9, San Diego, 2015.
- [11] H. Kannan, A. Kurakin, and I. Goodfellow, "Adversarial logit pairing," *arXiv:1803.06373*, 2018.
- [12] Y. Luo, X. Boix, G. Roig, T. Poggio, and Q. Zhao, "Foveation-based mechanisms alleviate adversarial examples," *arXiv:1511.06292*, 2015.
- [13] N. Papernot, P. D. McDaniel, X. Wu, S. Jha, and A. Swami, "Distillation as a defense to adversarial perturbations against deep neural networks," in *Proc. IEEE Symposium on Security and Privacy*, pp. 582–597, San Jose, 2016.
- [14] A. Madry, A. Makelov, L. Schmidt, D. Tsipras, and A. Vladu, "Towards deep learning models resistant to adversarial attacks," in *Proc. ICLR*, pp. 1–23, Vancouver, 2018.
- [15] I. Goodfellow, J. Shlens, and C. Szegedy, "Explaining and harnessing adversarial examples," in *Proc. ICLR*, pp. 1–11, San Diego, 2015.
- [16] P. Maini, E. Wong, and Z. Kolter, "Adversarial robustness against the union of multiple perturbation models," in *Proc. ICML*, pp. 6640–6650, 2020.
- [17] H. Zhang, Y. Yu, J. Jiao, E. Xing, L. El Ghaoui, and M. Jordan, "Theoretically principled trade-off between robustness and accuracy," in *Proc. ICML*, pp. 7472–7482, 2019.
- [18] T.-H. Chang, M. Hong, H.-T. Wai, X. Zhang, and S. Lu, "Distributed learning in the nonconvex world: From batch data to streaming and beyond," *IEEE Signal Processing Magazine*, vol. 37, no. 3, pp. 26–38, 2020.
- [19] A. H. Sayed, "Adaptive networks," *Proceedings of the IEEE*, vol. 102, no. 4, pp. 460–497, 2014.
- [20] A. H. Sayed, "Adaptation, learning, and optimization over networks," *Foundations and Trends in Machine Learning*, vol. 7, pp. 311–801, 2014.
- [21] C. Qin, J. Martens, S. Goyal, D. Krishnan, K. Dvijotham, A. Fawzi, S. De, R. Stanforth, and P. Kohli, "Adversarial robustness through local linearization," in *Proc. NeurIPS*, pp. 13824–13833, Vancouver, 2019.
- [22] G. Zhang, S. Lu, S. Liu, X. Chen, P.-Y. Chen, L. Martie, L. Horesh, and M. Hong, "Distributed adversarial training to robustify deep neural networks at scale," in *Proc. UAI*, pp. 2353–2363, Eindhoven, 2022.
- [23] Y. Liu, X. Chen, M. Cheng, C.-J. Hsieh, and Y. You, "Concurrent adversarial learning for large-batch training," in *Proc. ICLR*, pp. 1–17, 2022.
- [24] F. Feng, X. He, J. Tang, and T.-S. Chua, "Graph adversarial training: Dynamically regularizing based on graph structure," *IEEE Transactions on Knowledge and Data Engineering*, vol. 33, no. 6, pp. 2493–2504, 2021.
- [25] K. Xu, H. Chen, S. Liu, P. Y. Chen, T. W. Weng, M. Hong, and X. Lin, "Topology attack and defense for graph neural networks: An optimization perspective," in *Proc. IJCAI*, pp. 3961–3967, Macao, 2019.
- [26] X. Wang, X. Liu, and C.-J. Hsieh, "Graphdefense: Towards robust graph convolutional networks," *arXiv:1911.04429*, pp. 1–9, 2019.
- [27] A. Sinha, H. Namkoong, R. Volpi, and J. Duchi, "Certifying some distributional robustness with principled adversarial training," in *Proc. ICLR*, pp. 1–34, Vancouver, 2018.
- [28] Y. Wang, X. Ma, J. Bailey, J. Yi, B. Zhou, and Q. Gu, "On the convergence and robustness of adversarial training," in *Proc. ICML*, pp. 6586–6595, Long Beach, 2019.
- [29] D. Bertsekas, *Convex Optimization Theory*. Athena Scientific, 2009.
- [30] K. K. Thekumparampil, P. Jain, P. Netrapalli, and S. Oh, "Efficient algorithms for smooth minimax optimization," in *Proc. NeurIPS*, pp. 12659–12670, Vancouver 2019.
- [31] S. Vlaski and A. H. Sayed, "Distributed learning in non-convex environments—part I: Agreement at a linear rate," *IEEE Transactions on Signal Processing*, vol. 69, pp. 1242–1256, 2021.
- [32] S. Vlaski and A. H. Sayed, "Distributed learning in non-convex environments—part II: Polynomial escape from saddle-points," *IEEE Transactions on Signal Processing*, vol. 69, pp. 1257–1270, 2021.
- [33] T. Lin, C. Jin, and M. I. Jordan, "On gradient descent ascent for nonconvex-concave minimax problems," in *Proc. ICML*, pp. 6083–6093, 2020.
- [34] R. T. Rockafellar, *Convex Analysis*. Princeton University Press, 2015.
- [35] B. Ying and A. H. Sayed, "Performance limits of stochastic sub-gradient learning, Part II: Multi-agent case," *Signal Processing*, vol. 144, pp. 253–264, 2018.
- [36] J. Chen and A. H. Sayed, "On the learning behavior of adaptive networks - part I: Transient analysis," *IEEE Trans. Inf. Theory*, vol. 61, no. 6, pp. 3487–3517, 2015.
- [37] E. Wong, L. Rice, and J. Z. Kolter, "Fast is better than free: Revisiting adversarial training," in *Proc. ICLR*, pp. 1–17, Addis Ababa, 2020.
- [38] M. Kayaalp, S. Vlaski, and A. H. Sayed, "Dif-MAML: Decentralized multi-agent meta-learning," *IEEE Open Journal of Signal Processing*, vol. 3, pp. 71–93, 2022.
- [39] C. Jin, P. Netrapalli, and M. Jordan, "What is local optimality in nonconvex-nonconcave minimax optimization?," in *Proc. ICML*, pp. 4880–4889, 2020.
- [40] D. Davis and D. Drusvyatskiy, "Stochastic model-based minimization of weakly convex functions," *SIAM J. Optim.*, vol. 29, pp. 207–239, 2019.
- [41] L. Deng, "The MNIST database of handwritten digit images for machine learning research," *IEEE Signal Processing Magazine*, vol. 29, no. 6, pp. 141–142, 2012.
- [42] A. Krizhevsky and G. Hinton, "Learning multiple layers of features from tiny images," 2009. Technical Report.
- [43] S.-M. Moosavi-Dezfooli, A. Fawzi, and P. Frossard, "DeepFool: a simple and accurate method to fool deep neural networks," in *Proc. IEEE CVPR*, pp. 2574–2582, Las Vegas, 2016.
- [44] W. Brendel, J. Rauber, and M. Bethge, "Decision-based adversarial attacks: Reliable attacks against black-box machine learning models," in *Proc. ICLR*, pp. 1–12, Vancouver, 2018.
- [45] S. Ioffe and C. Szegedy, "Batch normalization: Accelerating deep network training by reducing internal covariate shift," in *Proc. ICML*, pp. 448–456, Lille, 2015.
- [46] H. Zhang, Y. Yu, J. Jiao, E. P. Xing, L. E. Ghaoui, and M. I. Jordan, "Theoretically principled trade-off between robustness and accuracy," in *Proc. ICML*, pp. 7472–7482, California, 2019.
- [47] N. Qian, "On the momentum term in gradient descent learning algorithms," *Neural Networks*, pp. 145–151, 1999.
- [48] M. Pintor, F. Roli, W. Brendel, and B. Biggio, "Fast minimum-norm adversarial attacks through adaptive norm constraints," in *Proc. NeurIPS*, pp. 20052–20062, 2021.
- [49] J. Rauber, W. Brendel, and M. Bethge, "Foolbox: A python toolbox to benchmark the robustness of machine learning models," in *Reliable Machine Learning in the Wild Workshop, ICML*, 2017.
- [50] T. Zhu, F. He, L. Zhang, Z. Niu, M. Song, and D. Tao, "Topology-aware generalization of decentralized SGD," in *Proc. ICML*, pp. 27479–27503, Baltimore, 2022.
- [51] N. S. Keskar, D. Mudigere, J. Nocedal, M. Smelyanskiy, and P. T. P. Tang, "On large-batch training for deep learning: Generalization gap and sharp minima," in *Proc. 5th ICLR*, pp. 1–16, Toulon, 2017.
- [52] T. Pang, M. Lin, X. Yang, J. Zhu, and S. Yan, "Robustness and accuracy could be reconcilable by (proper) definition," in *Proc. ICML*, pp. 17258–17277, Baltimore, 2022.
- [53] F. Tramèr and D. Boneh, "Adversarial training and robustness for multiple perturbations," in *Proc. NeurIPS*, pp. 5858–5868, Vancouver, 2019.